

# Li<sup>+</sup> solvation in pure, binary and ternary mixtures of organic carbonate electrolytes.

---

Ioannis Skarmoutsos<sup>†,\*</sup>, Veerapandian Ponnuchamy<sup>†</sup>, Valentina Vetere<sup>‡</sup>, Stefano Mossa<sup>†,\*</sup>

<sup>†</sup> Univ. Grenoble Alpes, INAC-SPRAM, F-38000 Grenoble, France; CNRS, INAC-SPRAM, F-38000 Grenoble, France and CEA, INAC-SPRAM, F-3800 Grenoble, France Emails: [ioannis.skarmoutsos@cea.fr](mailto:ioannis.skarmoutsos@cea.fr) , [stefano.mossa@cea.fr](mailto:stefano.mossa@cea.fr)

<sup>‡</sup> Univ. Grenoble Alpes, LITEN-DTNM, F-38000 Grenoble, France and CEA, LITEN-DTNM, F-38000 Grenoble, France

## Abstract

Classical molecular dynamics (MD) simulations and quantum chemical density functional theory (DFT) calculations have been employed in the present study to investigate the solvation of lithium cations in pure organic carbonate solvents (ethylene carbonate (EC), propylene carbonate (PC) and dimethyl carbonate (DMC)) and their binary (EC-DMC, 1:1 molar composition) and ternary (EC-DMC-PC, 1:1:3 molar composition) mixtures. The results obtained by both methods indicate that the formation of complexes with four solvent molecules around Li<sup>+</sup>, exhibiting a strong local tetrahedral order, is the most favorable. However, the molecular dynamics simulations have revealed the existence of significant structural heterogeneities, extended up to a length scale which is more than five times the size of the first coordination shell radius. Due to these significant structural fluctuations in the bulk liquid phases, the use of larger size clusters in DFT calculations has been suggested. Contrary to the findings of the DFT calculations on small isolated clusters, the MD simulations have predicted a preference of Li<sup>+</sup> to interact with DMC molecules within its first solvation shell and not with the highly polar EC and PC ones in the binary and ternary mixtures. This behavior has been attributed to the local tetrahedral packing of the solvent molecules in the first solvation shell of Li<sup>+</sup>, which causes a cancellation of the individual molecular dipole vectors and this effect seems to be more important in the cases where molecules of the same type are present. Due to these cancellation effects, the total dipole in the first solvation shell of Li<sup>+</sup> increases when the local mole fraction of DMC is high.

**Keywords:** Lithium ion, solvation, organic carbonates, battery electrolytes, molecular dynamics, density functional theory

## 1. Introduction

In recent years the demand for portable power applications has been highly increased, thus giving a considerable impetus to the development of novel electrochemical devices, such as electric double layer capacitors and lithium ion batteries. Lithium ion secondary batteries are very common in consumer electronics, such as laptop computers and cell phones, while they are also growing in popularity for automotive applications in order to decrease the green-house gas emissions in the atmosphere and, hence, to prevent global warming<sup>1-3</sup>. In general Li-ion batteries have been deployed so far in a wide-range of energy storage applications, ranging from energy-type batteries of a few kilowatt-hour in residential systems with rooftop photovoltaic arrays to multi-megawatt containerized ones, for the provision of grid ancillary services.

Li-ion cells mainly employ intercalation materials as positive and negative electrodes and aprotic electrolytes to conduct  $\text{Li}^+$ . The chemical nature of the electrodes determines the energy output, while the electrolyte affects the rate of the energy release by controlling mass transport properties within the battery<sup>1</sup>. The interactions between the electrolyte and the electrode materials are also very important and the formation of electrified interfaces between them often dictates the performance of the device. An electrolyte should meet a list of minimal requirements in order to be used in such devices. In general it should be a good ionic conductor and electronic insulator, have a wide electrochemical window, exhibit electrochemical, mechanical and thermal stability, be environmental friendly and inert to other cell components such as cell separators, electrode substrates, and cell packaging materials.

As mentioned above, the transport of  $\text{Li}^+$  ions inside the electrolyte determines the rate of the energy transfer, which has been stored on the electrodes<sup>4</sup>. According to the literature the transport of  $\text{Li}^+$  ions is controlled by a two-step mechanism involving the solvation of the ions by the solvent molecules, followed by the migration of the solvated ions<sup>5</sup>. A deeper understanding of the solvation of  $\text{Li}^+$  ions may therefore act as a springboard towards the rational design of novel electrolytes with improved  $\text{Li}^+$  conductivity.

By now, the most commonly employed strategy towards the rational design of electrolytes with optimal properties for battery applications is to use mixtures of cyclic and non-cyclic organic carbonates<sup>6</sup>. In such a way the high dielectric constant of cyclic carbonates is combined with the low viscosity of acyclic carbonates ensuring good performances under low temperature environments. On the other hand, the higher thermal stability of cyclic carbonates ensures a reasonable operating temperature range for the mixed solvent.

Although several experimental and theoretical studies devoted to the interactions of  $\text{Li}^+$  with pure and mixed carbonate-based electrolytes have already been published, the solvation structure and dynamics of lithium cations in these solvents is still a subject of debate. Interestingly, even the determination of the coordination number around the lithium ions in pure carbonate-based solvents has not been definitely resolved<sup>7-18</sup>. While the generally accepted picture comprises a tetrahedral coordination of the carbonyl oxygen atoms around  $\text{Li}^+$ , some experimental and theoretical studies propose the existence of local structures exhibiting slightly higher coordination numbers. The dependence of this local coordination number on the ion concentration is also somehow controversial. However, it should be emphasized that designing experimental methods or theoretical models to analyze the experimental data in order to provide a direct measurement of the coordination number is an extremely complicated topic<sup>7,19,20</sup>. On the other hand, since the validation of molecular simulation results strongly depends on the direct comparison with experimental data, the development of experimental methods proving a direct determination of the coordination number becomes indispensable in order to obtain a clear picture about the local structural effects in liquid solvents.

On the basis of the above considerations the aim of the present study is not to give a final answer to this particular problem. The main purpose is to provide some general insight concerning the differences in the solvation mechanisms of  $\text{Li}^+$  in pure and mixed binary and ternary carbonate-based solvents, by employing molecular dynamics simulations and quantum chemical calculations. Also, recent advances in the investigation of the local solvation structure by both means of experimental and theoretical techniques will be discussed and compared with the finding of the present study. Such a discussion might be used as a springboard towards a better

understanding of the solvation phenomena in these electrolytes, significantly improving the rational design of electrolytes for battery applications.

## **2. Computational Methods and Details**

### **2.1 Density Functional quantum chemical calculations**

Quantum chemical calculations for several clusters of pure, binary and ternary electrolytes including a lithium cation have been performed using the ADF software<sup>21</sup>. The Density Functional Theory (DFT) has been employed for the optimization of structures, using the PBE GGA<sup>22</sup> functional and a TZP (core double zeta, valence triple zeta, polarized) Slater type orbital (STO) basis set. Our calculations for some representative clusters have revealed that the basis set superposition error (BSSE) corrections<sup>23</sup> are negligibly small. A similar observation has also been pointed out in recent DFT studies<sup>24,25</sup>. Frequency analysis has been carried out for each structure ensuring the absence of imaginary modes, and confirming each structure as a minimum on the potential energy surface. Zero-point energy (ZPE) corrections have been also taken into account. Thermodynamic quantities such as the entropy, enthalpy and free energy of the investigated clusters have been estimated at the temperature of 298.15 K.

### **2.2 Molecular Dynamics Simulations**

In the present study the solvation structure of  $\text{Li}^+$  at infinite dilution in pure and mixed carbonate-based solvents has been investigated via classical molecular dynamics (MD) simulations. The selected pure solvents were ethylene carbonate (EC), propylene carbonate (PC) and dimethyl carbonate (DMC). The binary EC-DMC mixture with a molar composition 1 EC : 1 DMC and the ternary EC-DMC-PC one with 1 EC : 1 DMC : 3 PC molar composition were also studied.

Inside each simulation cubic box, one lithium cation was placed among 215 solvent molecules in the case of the pure solvents and the ternary mixture, whereas in the case of the binary mixture it was placed among 214 solvent molecules. Trial runs with larger system sizes have verified that the employed number of molecules are sufficient in describing the solvation structure of  $\text{Li}^+$ , avoiding in this way any

possible artifacts arising from finite size effects. The initial configurations of the simulated systems were prepared by using the *Packmol* software<sup>26</sup>.

The force fields employed in the simulations were adopted from previous studies<sup>27,28</sup>. The intermolecular interactions in these models are represented as pair wise additive with site-site 12-6 Lennard-Jones plus Coulomb interactions. The EC and PC molecules were kept rigid during the simulations (intramolecular geometries can be found in the Supporting Information). In the case of DMC, due to the existence of different conformers in the gas and liquid phase<sup>29-31</sup>, an intramolecular force field has been also employed. The intramolecular interactions have been represented in terms of harmonic angle bending and cosine series for dihedral angle internal rotations, whereas the bond lengths have been kept rigid by employing a modified version of the SHAKE<sup>32,33</sup> algorithm. The parameters of the intramolecular force field used are also presented in the Supporting Information. As pointed out in the introduction, the generally accepted picture comprises a tetrahedral coordination of the carbonyl oxygen atoms around  $\text{Li}^+$ . The potential models used in the presented study predict such local structures<sup>27,28</sup> and for this reason they were selected to be employed in the simulations. Results obtained with different potential models already published in the literature will be also discussed together with the findings of the present study.

The equations of motion were integrated using a leapfrog-type Verlet algorithm with an integration time step of 1 fs<sup>34</sup>. The temperature has been fixed to 303.15 K and the pressure to 1 atm by coupling the systems to a Nose-Hoover thermostat and barostat with relaxation times of 0.2 and 0.5 ps, respectively<sup>5,36</sup>. The rigid body equations of motion for EC and PC molecules were expressed in the quaternion formalism<sup>34</sup>. A cut-off radius of 9.0 Å has been applied for all Lennard-Jones interactions and long-range corrections have also been taken into account. To account for the long-range electrostatic interactions the standard Ewald summation technique has been used<sup>34</sup>. The simulation runs were performed using the DL\_POLY simulation code<sup>37</sup>. The systems were equilibrated for 25 ns and a subsequent run of 15 ns was performed in each case, in order to calculate equilibrium properties.

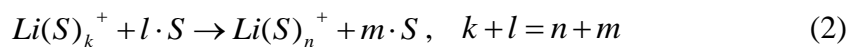
### 3. Results and Discussion

#### 3.1 Relative stability of isolated clusters

By employing DFT calculations, using the methodologies described in section 2.1, a wide range of clusters of the type  $\text{Li}(\text{S})_n^+$  (where  $\text{S}=\text{EC}, \text{PC}, \text{DMC}$  and  $n=1-5$ ) were optimized. Thermodynamic parameters, such as the enthalpy, entropy and binding energy of these clusters have been also estimated. The binding energies of these clusters have been expressed in terms of the equation:

$$\text{BE} = E(\text{Li}(\text{S})_n^+) - E(\text{Li}^+) - n E(\text{S}) \quad (1)$$

In order to provide an estimation of the preferable coordination number around the lithium cation, the most favorable path between these clusters  $\text{Li}(\text{S})_n^+$  has to be determined in terms of free energy changes. To do so, the free energies of the aggregates  $\text{Li}(\text{S})_n^+ + m \text{S}$  ( $n+m=\text{constant}=5$  in this case) were estimated, in order to define the aggregate exhibiting the lowest free energy value. In this way, if the fragment  $\text{Li}(\text{S})_n^+ + m \text{S}$  has the lowest free energy value, all paths of the type:



will exhibit a negative free energy change  $\Delta G$ , thus indicating that all possible paths leading to the cluster  $\text{Li}(\text{S})_n^+$  are favorable and, therefore, this cluster could be considered the most preferable one in terms of the free energy changes. Note that the paths depicted in Eq. 2 can correspond to both additions or subtractions of solvent molecules from one particular cluster leading to another, depending on the relative difference  $m-l$ . If  $m-l < 0$ , then the transition is being achieved through solvent addition, otherwise through solvent subtraction.

All the calculated values of enthalpy, entropy and binding energy of the investigated  $\text{Li}(\text{S})_n^+$  clusters, together with the free energy values of the  $\text{Li}(\text{S})_n^+ + m \text{S}$  aggregates are presented in Tables 1,2. From the results obtained it can be clearly seen that in the cases of EC and DMC, the predicted most favorable structures correspond to a tetracoordinated lithium cation. Similar conclusions have been drawn in the DFT study of Bhatt et al, studying the solvation of  $\text{Li}^+$  in EC<sup>24</sup>. In the case of PC the free energy difference for the path going from  $\text{Li}(\text{PC})_3^+$  to  $\text{Li}(\text{PC})_4^+$  is very small. This is an indication that although the  $\text{Li}(\text{PC})_3^+$  cluster has been predicted to be the most

favorable one, both structures could possibly exist in the bulk phase. The optimized structures for  $\text{Li}(\text{EC})_4^+$ ,  $\text{Li}(\text{PC})_3^+$  and  $\text{Li}(\text{PC})_4^+$ , as well as for  $\text{Li}(\text{DMC})_4^+$  are shown in Figures 1-3. From the data presented in Table 1 it might be also seen that in the cases of the tetracoordinated clusters the binding energies decrease in the order  $E(\text{Li}(\text{PC})_4^+) > E(\text{Li}(\text{EC})_4^+) > E(\text{Li}(\text{DMC})_4^+)$ , which is reasonable taking into account that the dipole moments of PC, EC and DMC molecules decrease in the same order (5.6, 5.3 and 0.35 D, respectively). It should be also noted that the entropic contributions to the free energy of each cluster exhibit the opposite trend, being more important in the case of the  $\text{Li}(\text{DMC})_4^+$ .

Considering that the tetracoordinated structure is the most preferable one, the same calculations have been performed for clusters of the type  $\text{Li}(\text{S}_1)_n(\text{S}_2)_m^+$ , where  $\text{S}_1=\text{EC}$ ,  $\text{S}_2=\text{DMC}$  and  $n+m=4$ . The free energy changes for the transitions:



where  $k+l=n+m=4$  and  $n,m,k,l=1-3$ , were also estimated, in order to find the most favorable structure among the clusters with two types of solvents around lithium. The calculated values of enthalpy, entropy and binding energy of the investigated  $\text{Li}(\text{S}_1)_n(\text{S}_2)_m^+$  clusters, together with the free energy values of the  $\text{Li}(\text{S}_1)_n(\text{S}_2)_m^+ + (4-n) \text{S}_1 + (4-m) \text{S}_2$  aggregates are presented in Tables 3,4. The results obtained reveal that among all the possible combinations of tetracoordinated clusters containing both EC and DMC the most preferable is  $\text{Li}(\text{EC})_3(\text{DMC})^+$ , followed by  $\text{Li}(\text{EC})_2(\text{DMC})_2^+$  and eventually the  $\text{Li}(\text{EC})(\text{DMC})_3^+$  is the least favorable among these three clusters. This finding is in agreement with both ab initio studies by Borodin and Smith<sup>38</sup>, where the relative stabilities were based upon the energies of the complexes, and with the very recently reported study by Bhatt and O'Dwyer<sup>25</sup>. The structures of the optimized clusters are presented in Figure 4.

Finally, a similar analysis was performed for the clusters  $\text{Li}(\text{S}_1)_n(\text{S}_2)_l(\text{S}_3)_m^+$  ( $\text{S}_1=\text{EC}$ ,  $\text{S}_2=\text{DMC}$ ,  $\text{S}_3=\text{PC}$ ), containing EC, DMC and PC solvent molecules. The structures of the optimized clusters are presented in Figure 5. From the results obtained using the same methodology discussed above, which are presented in Tables 5,6, it can be seen that the cluster  $\text{Li}(\text{EC})_2(\text{DMC})(\text{PC})^+$ , seems to be the most favorable one, followed by  $\text{Li}(\text{EC})(\text{DMC})(\text{PC})_2^+$  and finally by  $\text{Li}(\text{EC})(\text{DMC})_2(\text{PC})^+$ . However the free energy

changes for the transition paths between these clusters are very small, indicating that all these structures could possibly exist in the bulk phase. Also the free energy changes for the transition paths leading to the  $\text{Li}(\text{EC})_4^+$  and  $\text{Li}(\text{PC})_4^+$  clusters are very small. Interestingly, it has also been found that the transitions from clusters containing only EC and DMC to clusters with three types of solvent molecules, by substitution of one EC or DMC molecule with a PC one, are favorable in terms of the free energy changes. The substitution of a DMC molecule has been found to be more favorable than the substitution of an EC one. In general the above findings indicate that the presence of PC contributes to the stabilization of the clusters. This fact can be also supported by the calculated binding energies of the tetracoordinated clusters, which are plotted together in Figure 6.

Interestingly, from Tables 4,6 it can also be seen that the presence of DMC contributes to the increase of the entropy and therefore to the decrease of the free energy of the clusters containing more than one solvent type. Therefore, although from an energetic point of view the preference of  $\text{Li}^+$  to bind with the highly polar PC and EC molecules is undoubtful, from an entropic point of view the addition of DMC molecules contributes to the decrease of the free energy of the clusters. In the investigated finite size clusters the energetic contribution seems to be the most important one. However, the small free energy differences observed for the transition paths leading from one cluster to the other indicate that the formation of these clusters should be investigated at more extended length scales, in order to have a more realistic description of the effects taking place in the bulk liquid phase. This was the most important motivation to combine DFT calculations of isolated clusters with classical MD simulations at more extended length scales, in order to have a clearer picture about the solvation of  $\text{Li}^+$  in pure and mixed organic carbonate-based solvents.

### 3.2 Liquid Solvation Structure

By analyzing the trajectories obtained by the classical MD simulations described in section 2.2, the local structure around  $\text{Li}^+$  were investigated for all the selected pure and mixed solvents. The local structure was analyzed in terms of the most representative atom-atom pair radial distribution functions (prdf). The results obtained indicate a preferential interaction of  $\text{Li}^+$  with the carbonyl oxygen atom ( $\text{O}_\text{C}$ ) of the carbonate molecules, which is in agreement with all the previously reported



experimental and theoretical studies. The calculated  $\text{Li}^+\text{-O}_\text{C}$  prdfs between  $\text{Li}^+$  and the carbonyl oxygen atoms of EC, PC and DMC in the pure, binary and ternary solvents are presented in Figure 7.

One of the main features of the calculated prdfs is the existence of a high intensity peak located at 1.8 Å in all cases. In the cases of the pure solvents the amplitude of this first peak decreases in the order  $\text{DMC} > \text{PC} > \text{EC}$ . In the cases of the binary and ternary mixtures, the amplitude increases significantly in the case of DMC and decreases in the cases of EC and PC. The high amplitude of the first peak of the  $\text{Li}^+\text{-O}_\text{C}$  prdf in the case of DMC indicates a strong interaction between  $\text{Li}^+$  and the DMC molecules. The position of the first minimum, which determines the size of the first solvation shell, is located at about 2.6 Å in the case of the pure solvents and the binary mixture and at about 2.4 Å in the case of the ternary one. In order to estimate the number of solvent molecules around  $\text{Li}^+$  in all the investigated systems, the local coordination numbers of each type of solvent were calculated as a function of the distance from the lithium cation and they are presented in Figure 8. The values of the peak positions and amplitudes of the calculated prdfs, together with the first minimum position and the corresponding coordination numbers for the first solvation shell are presented in Table 7.

From all these data it can be concluded that the solvation shell of  $\text{Li}^+$  consists of four solvent molecules and this situation does not change in the cases of the binary and ternary solvent mixtures. At this point it should be mentioned that several MD simulation studies<sup>27,28,38-45</sup> of the solvation of  $\text{Li}^+$  in pure carbonate solvents have given different estimations of the coordination number corresponding to the first solvation shell of  $\text{Li}^+$ . In particular, whereas some potential models predict a solvation shell of  $\text{Li}^+$  which consists of four solvent molecules<sup>27,28,38-40</sup>, other force fields predict a higher coordination number<sup>41,43</sup>. The potential models predicting higher coordination numbers also exhibit a strong dependence of the obtained coordination number on the salt concentration. From the shape of the obtained prdfs it is also clear that there are significant local structural inhomogeneities in the system. These structural fluctuations are reflected on the behavior of the prdfs, which reveal the presence of well-structured second and third coordination shells. Eventually they reach the homogeneous limit, obtaining values close to unity, only at length scales longer than 15 Å.

In the cases of mixtures of organic carbonate solvents only a limited number of studies<sup>38,43,46</sup> have focused on the solvation of  $\text{Li}^+$  in binary mixtures. Also, to the best of our knowledge, this is the first simulation study devoted to the solvation of  $\text{Li}^+$  in ternary mixtures of carbonate-based solvents. In binary and ternary mixtures, beyond the estimation of the coordination number of the primary solvation shell around lithium the mixed composition of the shell is also of interest. The local compositional fluctuations in a spherical shell around  $\text{Li}^+$  can be characterized in terms of the corresponding local mole fractions of each type of solvent<sup>47</sup>. For instance, in a ternary mixture of solvents with indices  $i, j, k$  the local mole fraction of solvent  $k$  around  $\text{Li}^+$  is expressed as:

$$X_k(r) = \frac{n_k(r)}{n_i(r) + n_j(r) + n_k(r)} \quad (4)$$

In Eq. 4,  $n_k(r)$  is the coordination number of solvent  $k$  corresponding to a spherical shell of radius  $r$  around  $\text{Li}^+$ . In a similar way, all the local mole fractions for the different types of solvents in the binary and ternary mixture around  $\text{Li}^+$  have been calculated and are presented in Figure 9. The coordination number considered in the present calculations corresponds to the carbonyl oxygen atoms of each solvent around  $\text{Li}^+$ . The results obtained from the present MD simulations actually reveal that in the cases of binary and ternary mixtures there is a high concentration of DMC in the first solvation shell of  $\text{Li}^+$ . The existence of significant compositional fluctuations around  $\text{Li}^+$  can also be observed. As a result of these fluctuations, the structure around  $\text{Li}^+$  could be described in terms of a short-range structure (up to 4-5 Å from  $\text{Li}^+$ ) where the composition is rich in DMC, and by a longer-range structure where in the case of the binary solvent mixture the composition is rich in EC and, in the case of the ternary one, it is rich in PC. At larger length scales, in the range of about 15 Å from the lithium cation, the local mole fractions of each solvent reach the corresponding bulk value. From Figure 9 it can also be observed that the typical length scale of these fluctuations around  $\text{Li}^+$  is slightly more extended in the case of the ternary mixture than in the binary one.

From a first instance the findings of the MD simulations regarding the composition of the first solvation shell of  $\text{Li}^+$  in binary and ternary mixtures seem to be in contradiction with the results obtained by the DFT calculations. However, it should be

pointed out that the first shell structure predicted in the MD simulations could be the result of local structural correlations between the first, second and third solvation shells which exhibit completely different compositions. Indeed, the collective effects arising due to the interactions between regions of different density and composition could possibly stabilize the local structure observed inside the first solvation shell of  $\text{Li}^+$ . These are clearly not taken into account in the cases of the DFT calculations, where isolated clusters have been investigated. To perform a meaningful comparison between MD and DFT results in cases where significant structural fluctuations are present, extended far beyond the first solvation shell, the use of larger size clusters in DFT calculations seems to be needed.

To obtain a more detailed picture of the multiple different local microstructures observed in the first solvation shell of  $\text{Li}^+$ , an analysis of the different clusters  $\text{Li}(\text{S}_1)_n(\text{S}_2)_l(\text{S}_3)_m^+$  ( $\text{S}_1=\text{EC}$ ,  $\text{S}_2=\text{DMC}$ ,  $\text{S}_3=\text{PC}$ ,  $n,l,m= 0 - 4$  and  $n+l+m=4$ ) observed inside this shell was performed for the binary and ternary solvent mixtures. The relative populations of these are shown in Figure 10. In the binary mixture, the most prominent clusters inside the first solvation of  $\text{Li}^+$  are the  $\text{Li}(\text{EC})(\text{DMC})_3^+$  and the  $\text{Li}(\text{EC})_2(\text{DMC})_2^+$ , with the first exhibiting almost double occurrence probability. There is also a small fraction of clusters (7.2 %) where  $\text{Li}^+$  is pentacoordinated. About 80 % of these 5-coordinated  $\text{Li}^+$  complexes consist of 2 EC and 3 DMC molecules, 19 % of 3 EC and 2 DMC molecules and an almost negligible 1 % fraction consists of 1 EC and 4 DMC molecules. In the ternary mixture the most prominent clusters are  $\text{Li}(\text{EC})(\text{DMC})_2(\text{PC})^+$  and  $\text{Li}(\text{DMC})_2(\text{PC})_2^+$ , having though non-negligible fractions of  $\text{Li}(\text{EC})(\text{DMC})(\text{PC})_2^+$ ,  $\text{Li}(\text{DMC})_3(\text{PC})^+$ ,  $\text{Li}(\text{DMC})(\text{PC})_3^+$  and a smaller one corresponding to the  $\text{Li}(\text{EC})_2(\text{DMC})_2^+$  cluster. It should be noted that almost half of the observed clusters with four solvent molecules (49.7 %) do not contain EC at all, whereas DMC is involved in the formation of all of them. PC is absent in only 6.2 % of the total fraction of clusters with four solvent molecules. There is also a fraction 5.75 % of clusters with five solvent molecules and an almost negligible one (0.25 %) of clusters where  $\text{Li}^+$  is hexacoordinated.

Interestingly, such a discrepancy between the results obtained by MD and DFT calculations has been also reported by Borodin and Smith<sup>38</sup>. In their study, Borodin and Smith performed a MD simulation of a solution of  $\text{LiPF}_6$  in an equimolar EC-DMC binary mixture (EC+DMC:Li=11.8) using a polarizable potential model. The

coordination number of DMC in the first solvation shell of  $\text{Li}^+$  was higher than the coordination number of EC. This is in contrast with the results reported by Tenney and Cygan<sup>43</sup>, favoring the presence of EC in the first solvation shell of  $\text{Li}^+$  in a low concentration  $\text{LiPF}_6$  solution in a binary equimolar EC-DMC mixture. However, there is a significant difference between the potential models employed in these two MD simulation studies. The potential model used by Borodin and Smith<sup>38</sup> mainly predicts tetracoordinated  $\text{Li}^+$  complexes inside its first solvation shell, whereas in the case of the simulation reported by Tenney and Cygan<sup>43</sup> the solvation shell of  $\text{Li}^+$  mainly consists of five or six solvent molecules. The potential model used in the presented study also favors local structures with four solvent molecules around  $\text{Li}^+$ . This observation was an additional motivation to search for possible correlations between the formation of a local tetrahedral structure and the preference of  $\text{Li}^+$  to form a first solvation shell mainly consisting of DMC molecules.

The local tetrahedral structure around lithium can be investigated in terms of the tetrahedral order parameter,  $q$ <sup>48</sup>. This parameter  $q$  provides information about the extent to which a particle and its four nearest neighbors adopt a tetrahedral arrangement and is defined as:

$$q = 1 - \left\langle \frac{3}{8} \sum_{j=1}^3 \sum_{k=j+1}^4 \left( \cos \phi_{jik} + \frac{1}{3} \right)^2 \right\rangle \quad (5)$$

In this equation  $\phi_{jik}$  corresponds to the angle formed by the vectors  $\vec{r}_{ij}$  and  $\vec{r}_{ik}$ , connecting the lithium cation  $i$  with the oxygen atoms of two of its four nearest neighbours  $j, k$ . Using this definition,  $q=1$  in a perfect tetrahedral network and  $q=0$  in an ideal gas<sup>48</sup>. Kumar et al<sup>49</sup> have also suggested that an entropic term associated with this local tetrahedral order around a particle can be calculated from the probability distribution of the tetrahedral order parameter  $P(q)$ :

$$S_{\text{tet}} = \frac{3}{2} \cdot K_B \int \ln (1-q) \cdot P(q) \cdot dq \quad (6)$$

The normalized distributions  $P(q)$  have been calculated for all the simulated systems and are presented in Figure 11. The average values of  $q$  and  $S_{\text{tet}}$  are shown in Table 8.

From the shape of these distributions it can be seen that there is a very significant tetrahedral local ordering around  $\text{Li}^+$  in all cases and the addition of cosolvents does not significantly distort this structural order. The average values of  $q$  are in the range of about 0.93-0.96 in all cases, very close to the ideal tetrahedron value. Whereas there is no significant difference in the average values of  $q$ , the calculated value of  $S_{\text{tetr}}$  is noticeably lower in the case of the pure DMC solution, signifying that from an entropic point of view the presence of DMC contributes to the stabilization of the local tetrahedral structure around  $\text{Li}^+$ .

As it has been pointed out by one of the Authors in a previous publication<sup>50</sup>, given the additive property of the integral in Eq. 6, the contributions of different cluster structures to the calculated  $S_{\text{tetr}}$  value can be easily extracted. By using the fractions  $\chi_{nlm}$  of the different cluster structures  $\text{Li}(\text{S}_1)_n(\text{S}_2)_l(\text{S}_3)_m^+$  ( $\text{S}_1=\text{EC}$ ,  $\text{S}_2=\text{DMC}$ ,  $\text{S}_3=\text{PC}$ ), already depicted in Figure 10, the tetrahedral entropic term  $S_{\text{tetr}}$  per lithium cation is

given by  $S_{\text{tetr}} = \sum_{nlm} \chi_{nlm} \cdot S_{\text{tetr}}^{nlm}$ , where the contribution of each cluster state is:

$$S_{\text{tetr}}^{nlm} = \frac{3}{2} \cdot K_B \int \ln(1-q) \cdot P^{nlm}(q) \cdot dq \quad (7)$$

In this equation  $P^{nlm}(q)$  is the normalized probability density distribution of the tetrahedral order parameter  $q$  corresponding to a cluster  $\text{Li}(\text{S}_1)_n(\text{S}_2)_l(\text{S}_3)_m^+$  inside the first solvation shell of  $\text{Li}^+$ . The calculated values of  $S_{\text{tetr}}^{nlm}$  corresponding to all the tetracoordinated  $\text{Li}^+$  clusters observed during the simulations of the dilute solutions of  $\text{Li}^+$  in the pure, binary and ternary solvents are presented in Figure 12. In general it can be observed that the clusters having a high fraction of DMC molecules (3 and 4 molecules) exhibit a higher tetrahedrality, which is reflected in the lower values of  $S_{\text{tetr}}^{nlm}$ . Interestingly there is also a small difference in the  $S_{\text{tetr}}^{nlm}$  values of the clusters  $\text{Li}(\text{EC})_2(\text{DMC})_2^+$  observed in the binary and ternary solvent mixtures, the  $\text{Li}(\text{EC})_2(\text{DMC})_{2(b)}^+$  and  $\text{Li}(\text{EC})_2(\text{DMC})_{2(t)}^+$  clusters, respectively. This is a clear indication of the effect of the second solvation shell structure, which is different in the binary and ternary solvent mixtures, on the stabilization of the local structure observed in the first solvation shell. This observation further supports our previous statements that the use of larger size clusters in DFT calculations is required in cases

where there are significant structural fluctuations, extended far beyond the first solvation shell.

It should be mentioned that previous experimental studies, using electrospray ionization and mass spectrometry (ESI-MS) techniques<sup>51</sup>, have predicted a stronger preference of  $\text{Li}^+$  to bind with EC than with DMC in binary EC-DMC solvents. This preference has been attributed to the stronger ion dipole interactions between  $\text{Li}^+$  and EC molecules. However, the authors in that study pointed out that their results have been extracted from measurements of isolated clusters formed by two solvent molecules only instead of four. This difference has been attributed to the relative depletion of free solvent molecules at high salt concentrations or to a possible partial desolvation, during which the loosely bound molecules in the  $\text{Li}(\text{S})_4^+$  clusters (S: solvent) could be lost before the solvated species ever reach the aperture of the spectrometer.

Borodin and Smith<sup>38,52</sup> pointed out in their study, where they observed a slight preference for  $\text{Li}^+$  to bind with DMC, that the composition of the  $\text{Li}^+$  solvation can be different in the gas and liquid phases. Takeuchi et al.<sup>40</sup> have come to similar conclusions about the  $\text{Li}^+$  binding patterns to a  $\text{PF}_6^-$  anion. Another issue, which has not been discussed in the previous ESI-MS investigation, is the importance of the presence of the anions in the stabilization of the  $\text{Li}^+$  solvation shell. The investigated solutions had a high salt concentration and therefore the presence of the anions could strongly affect the preferential binding of  $\text{Li}^+$  with the solvent molecules. The preferential solvation around  $\text{Li}^+$  in binary and ternary mixtures is a quite complicated issue and besides the relative permittivity and donicity of the cyclic and acyclic components of the mixed solvent<sup>51</sup>, the salt concentration possibly plays a very important role. This statement is also supported by the findings of Borodin and Smith<sup>38</sup>, where the presence or not of  $\text{PF}_6^-$  anions in the solvation shell around  $\text{Li}^+$  strongly affects the preferential binding of  $\text{Li}^+$  with the cyclic and acyclic solvent molecules. This was the main reason why in the presented study dilute solution of  $\text{Li}^+$  were selected to be investigated, to focus more on the effects arising just due to the individual cation-solvent and solvent-solvent interactions. However, the anion concentration effect on the local solvation structure of mixed electrolyte solvents is a very important topic and will be the subject of a forthcoming study.

In general the preferential solvation around  $\text{Li}^+$  is being discussed in terms of the strength of individual pair cation-dipole interactions. In this sense, the observed

preferential solvation of  $\text{Li}^+$  by the non-polar DMC molecules instead of the highly polar EC and PC molecules seems to be problematic. To obtain a deeper insight, having in mind that collective effects might play a very important role in the solvation phenomena in condensed phases, the total dipole of the solvent molecules inside the solvation shell of  $\text{Li}^+$  were calculated:

$$\vec{M}_{sh} = \sum_i \vec{\mu}_i, \text{ with } r_{i-\text{Li}} \leq r_c \quad (8)$$

In Eq. 8,  $r_c = 2.6 \text{ \AA}$  is the distance determining the size of the solvation shell taken into account in the calculations. The calculated normalized probability density distributions  $P(M_{sh})$  of the magnitude of the total dipole  $M_{sh} = |\vec{M}_{sh}|$  for all the investigated systems are presented in Figure 13. From these data it is clear that inside the first solvation shell of  $\text{Li}^+$  in ternary and binary mixtures, which exhibits a high concentration of non-polar DMC molecules, the total dipole of the solvent molecules is higher than in the cases where  $\text{Li}^+$  is solvated by the highly polar EC and PC molecules. This finding signifies that the observed tetrahedral arrangement of the solvent molecules inside the solvation shell of  $\text{Li}^+$  causes a cancellation of the individual molecular dipole vectors and this cancellation is more important in the cases where molecules of the same geometry are present. When different types of solvent molecules are tetrahedrally packed inside the first solvation the resulting total dipole is higher, even though the fraction of the non-polar DMC molecules is higher.. As a result, the local environment around  $\text{Li}^+$  becomes more polar when the fraction of DMC is higher. This observation clearly indicates that collective effects are very important in determining the local dielectric environment around a  $\text{Li}^+$  cation and the relative binding preferences should be determined on the basis of this collective dipole moment of the solvation shell and not in terms of pair ion-dipole interactions. Before closing this section it would be useful to point out again that the experimental determination of the coordination number around the lithium ions in pure carbonate-based solvents has not been definitely resolved<sup>7-18</sup>. As it was mentioned in the introduction, it should be however emphasized that designing experimental methods or theoretical models to analyze the experimental data in order to provide a direct measurement of the coordination number is an extremely complicated topic<sup>7,19,20</sup>. Nevertheless, it seems that recent advances<sup>53</sup> in the field of coupling theoretical methods with experiments to bias molecular simulations with experimental data tend

to favor a tetrahedral-like structure, as also sophisticated polarizable models<sup>38</sup>, which predict a wide range of properties very close to the experimental ones. And this was the main reason why a simple model, predicting a tetrahedral network around  $\text{Li}^+$ , was selected in the present treatment. In general, one of the most reliable experimental methods to extract information about the local structure in liquids is neutron diffraction. Only one neutron diffraction study of a 10 mol % solution of  $\text{LiPF}_6$  in liquid PC has been reported up to now<sup>12</sup>. In this study the authors, by integrating the total radial distribution function  $G(r)$  obtained by the diffraction experiments up to its first minimum, have estimated the coordination number around  $\text{Li}^+$  to be 4.5. However, they have assumed that all the contributions to the total  $G(r)$  at the short-range part up to 2.4 Å arise from the  $\text{Li}^+\text{-O}_c$  prdf. By inspecting the above mentioned theoretical studies<sup>38,53</sup> and by performing a trial simulation of the same system, it became obvious that the  $\text{Li}^+\text{-F}$  prdf contributes to the shape of the total  $G(r)$  at this short-range. Therefore, a part of this 4.5 coordination number arises from the  $\text{Li}^+\text{-F}$  coordination number. But the cation-anion coordination number at the same range is definitely smaller, since the  $\text{Li}^+\text{-F}$  prdf and corresponding coordination number provide information about the number of fluorine atoms inside the solvation shell of  $\text{Li}^+$ , which of course could belong to the same  $\text{PF}_6^-$  anion. So, it is very likely that the coordination number giving the total number of solvent molecules and anions around  $\text{Li}^+$  should be smaller and could be even closer to four, or less. However, from that neutron diffraction study it's not possible to extract the separate contributions of the  $\text{Li}^+\text{-O}_c$  and  $\text{Li}^+\text{-F}$  prdfs in order to have a more accurate estimation of the total coordination number in the first solvation shell of  $\text{Li}^+$ . From this observation it becomes clear that even the interpretation of experimental data should be treated very carefully and if it is also combined with reverse modeling techniques<sup>54</sup> it could provide even more valuable information.

#### 4. Concluding Remarks

In the present study the solvation of  $\text{Li}^+$  in pure carbonate-based solvents and their binary and ternary mixtures has been investigated using a combination of quantum chemical DFT calculations and classical MD simulations. An analysis based on the changes in the free energy associated to the transitions between different types of clusters formed by the lithium cation and the solvent molecules has shown that the



formation of complexes with four solvent molecules is the most favorable. In the cases of clusters containing EC and DMC molecules, the DFT calculations have predicted a preferential binding with EC rather than with DMC. For the clusters having at the same type EC, PC and DMC molecules, although the  $\text{Li}(\text{EC})_2(\text{DMC})(\text{PC})^+$  has been predicted to be the most favorable one, the free energy changes for the transition paths between several clusters are very small, indicating that all these structures could possibly exist in the bulk phase.

On the other hand the MD simulations have revealed the existence of significant structural heterogeneities, extended up to a length scale which is more than five times the size of the first shell radius. These heterogeneities are very important in the cases of the binary and ternary solvent mixtures, revealing very significant compositional inhomogeneities around a lithium cation. As a result of these fluctuations, the structure around  $\text{Li}^+$  in the mixed solvents could be described in terms of a short-range structure (up to 4-5 Å from  $\text{Li}^+$ ) where the composition is rich in DMC and by a longer-range structure where in the case of the binary solvent mixture the composition is rich in EC and in the case of the ternary one it is rich in PC. The local mole fractions of each solvent obtain their bulk values at more extended length scales, as it was mentioned above. Such a finding indicates that the collective effects arising due to the interactions between regions of different composition could possibly stabilize the local structure of the first solvation shell of  $\text{Li}^+$ .

In the DFT calculations of the finite size isolated clusters, although from an energetic point of view the preference of  $\text{Li}^+$  to bind with the highly polar PC and EC molecules is undoubtful, from an entropic point of view the addition of DMC molecules contributes to the decrease of the free energy of the clusters. In these finite size clusters the energetic contribution seems to be the most important one. However, the small free energy differences observed for the transition paths leading from one cluster to the other indicate that the formation of these clusters should be investigated at more extended length scales in order to have a more realistic description of the effects taking place in the bulk liquid phase. The existence of significant structural fluctuations in the bulk liquid phases, extended far beyond the first solvation shell, signifies that to achieve a direct comparison between the MD and the DFT results the use of larger size clusters in DFT calculations seems to be more appropriate.

The MD simulations have also revealed that there is a very significant tetrahedral local ordering around  $\text{Li}^+$  in all cases and the addition of cosolvents does not distort this structural order. By calculating an entropic term associated with this local tetrahedral order around  $\text{Li}^+$ , it has also been revealed that the clusters having a high fraction of DMC molecules (3 and 4 molecules) exhibit a higher tetrahedrality, which is reflected in the lower values of this entropic term. Therefore, from an entropic point of view the presence of DMC contributes to the stabilization of the local tetrahedral structure around  $\text{Li}^+$ .

A very interesting finding also revealed in the present study is that inside the first solvation shell of  $\text{Li}^+$  in the ternary and binary mixtures, which exhibit a high concentration of non-polar DMC molecules, the total dipole of the solvent molecules is higher than in the cases where  $\text{Li}^+$  is solvated by the highly polar EC and PC molecules. The observed local tetrahedral packing of the solvent molecules in the first solvation shell of  $\text{Li}^+$  causes a cancellation of the individual molecular dipole vectors, which seems to be more important in the cases where molecules of the same type are present. These collective effects are very important in determining the local permittivity around a  $\text{Li}^+$  cation and the relative binding preferences should be based upon this total dipole moment of the solvation shell and not in terms of the pair ion-dipole interactions, which is traditionally considered as the most important factor determining the preferential solvation in such systems.

### **Acknowledgements:**

The authors acknowledge financial support from ANR-2011 PRGE002-04 ALIBABA and DSM Energie CEA Program.

### **Supporting Information Available:**

The details of the inter- and intra-molecular classical force fields employed in the present study are provided in the Supporting Information as a DL-POLY FIELD file.

## References

- 1) Xu, K. Nonaqueous Liquid Electrolytes for Lithium-based Rechargeable Batteries. *Chem. Rev.* **2004**, *104*, 4303
- 2) Armand, M.; Tarascon, J. M. Building Better Batteries. *Nature* **2008**, *541*, 652
- 3) Kim, Y.; Goodenough, J. B. Challenges for Rechargeable Li Batteries. *Chem. Mater.* **2010**, *22*, 587
- 4) Besenhard, J.O.; Winter, M.; Yang, J.; Biberacher, W. Filming Mechanism of Lithium-Carbon Anodes in Organic and Inorganic Electrolytes. *J. Power Sources* **2005**, *54*, 228
- 5) Yuan, K.; Bian, H.; Shen, Y.; Jiang, B.; Li, J.; Zhang, Y.; Chen, H.; Zheng, J. Coordination Number of  $\text{Li}^+$  in Nonaqueous Electrolyte Solutions Determined by Molecular Rotational Measurements. *J. Phys. Chem. B* **2014**, *118*, 3689
- 6) Eshetu, G. G.; Bertrand, J.P.; Lecocq, A.; Grugeon, S.; Laruelle, S.; Armand, M.; Marlair, G. Fire behavior of carbonates-based electrolytes used in rechargeable batteries with a focus on the role of the  $\text{LiPF}_6$  and  $\text{LiFSI}$  salts. *J. Power Sources* **2014**, *269*, 804
- 7) Bogle, X.; Vazquez, R.; Greenbaum, S.; von Wald Cresce, A.; Xu, K. Understanding  $\text{Li}^+$ - Solvent Interaction in Nonaqueous Carbonate Electrolytes with  $^{17}\text{O}$  NMR. *J. Phys. Chem. Lett.* **2013**, *4*, 1664-1668
- 8) Castriota, M.; Cazzanelli, E.; Nicotera, I.; Coppola, L.; Oliviero, C.; Ranieri, G.A. Temperature dependence of lithium ion solvation in ethylene carbonate- $\text{LiClO}_4$  solutions. *J. Chem. Phys.* **2003**, *118*, 5537-5541
- 9) Yuan, K.; Bian, H.; Shen, Y.; Jiang, B.; Li, J.; Zhang, Y.; Chen, H.; Zheng, J. Coordination Number of  $\text{Li}^+$  in Nonaqueous Electrolyte Solutions Determined by Molecular Rotational Measurements. *J. Phys. Chem. B* **2014**, *118*, 3689-3695
- 10) Xu, K.; Lam, Y.; Zhang, S.S.; Jow, T. R.; Curtis, T.B. Solvation Sheath of  $\text{Li}^+$  in Nonaqueous Electrolytes and Its Implication of Graphite/Electrolyte Interface Chemistry. *J. Phys. Chem. C* **2007**, *111*, 7411-7421

- 11) Smith, J. W.; Lam, R.K.; Sheardly, A.T.; Shih, O.; Rizzuto, A.M.; Borodin, O.; Harris, S.J.; Prendergast, D.; Saykally, R.J. X-Ray absorption spectroscopy of  $\text{LiBF}_4$  in propylene carbonate: a model lithium ion battery electrolyte. *Phys. Chem. Chem. Phys.* **2014**, DOI: 10.1039/c4cp03240c
- 12) Kameda, Y.; Umebayashi, Y.; Takeuchi, M.; Wahab, M.A.; Fukuda, S.; Ishiguro, S.; Sasaki, M.; Amo, Y.; Usuki, T. Solvation structure of  $\text{Li}^+$  in concentrated  $\text{LiPF}_6$ -propylene carbonate solutions. *J. Phys. Chem. B* **2007**, *111*, 6104-6109
- 13) Morita, M.; Asai, Y.; Yoshimoto, N.; Ishikawa, M. A Raman spectroscopic study of organic electrolyte solutions based on binary solvent systems of ethylene carbonate with low viscosity solvents which dissolve different lithium salts. *J. Chem. Soc. Faraday Trans.* **1998**, *94*, 3451-3456
- 14) Tsunekawa, H.; Narumi, A.; Sano, M.; Hiwara, A.; Fujita, M.; Yokoyama, H. Solvation and Ion Association Studies of  $\text{LiBF}_4$ -Propylenecarbonate-Trimethyl Phosphate Solutions. *J. Phys. Chem. B* **2003**, *107*, 10962-10966
- 15) Nie, M.; Abraham, D.P.; Seo, D.M.; Chen, Y.; Bose, A.; Lucht, B.L. Role of Solution Structure in Solid Electrolyte Interphase Formation on Graphite with  $\text{LiPF}_6$  in Propylene Carbonate. *J. Phys. Chem. C* **2013**, *117*, 25381-25389
- 16) Li, Y.; Xiao, A.; Lucht, B.L. Investigation of solvation in lithium ion battery electrolytes by NMR spectroscopy. *J. Mol. Liq.* **2010**, *154*, 131-133
- 17) Kondo, K.; Sano, M.; Hiwara, A.; Takehiko, O.; Fujita, M.; Kuwae, A.; Iida, M.; Mogi, K.; Yokoyama, H. Conductivity and Solvation of  $\text{Li}^+$  Ions of  $\text{LiPF}_6$  in Propylene Carbonate Solutions. *J. Phys. Chem. B* **2000**, *104*, 5040-5044
- 18) Barthel, J.; Buchner, R.; Wismeth, E. FTIR Spectroscopy of Ion Solvation of  $\text{LiClO}_4$  and  $\text{LiSCN}$  in Acetonitrile, Benzonitrile and Propylene Carbonate. *J. Solution Chem.* **2000**, *29*, 937-954
- 19) Buchner, R. Dielectric Spectroscopy of Solutions. In *Novel Approaches to the Structure and Dynamics of Liquids: Experiments, Theories and Simulations*; Samios J.; Durov, V.A. Eds.; Kluwer Academic Publishers; 2004; p 265.

- 20) Ravel, B.; Kelly, S.D. The Difficult Chore of Measuring Coordination by EXAFS *AIP Conf. Proc.* **2007**, 882, 150-152
- 21) te Velde, G.; Bickelhaupt, F.M.; van Gisbergen, S.J.A.; Fonseca Guerra, C.; Baerends, E.J.; Snijders, J.G.; Ziegler, T. Chemistry with ADF. *J. Comput. Chem.* **2001**, 22, 931-967
- 22) Perdew, J.P.; Burke, K.; Ernzerhof, M. Generalized gradient approximation made simple. *Phys. Rev. Lett.* **1996**, 77, 3865-3868
- 23) Boys, S.F.; Bernardi, F. Calculation of Small Molecular Interactions by Differences of Separate Total Energies – Some Procedures with Reduced Errors. *Mol. Phys.* **1970**, 19, 553
- 24) Bhatt, M.D.; Cho, M.; Cho, K. Interaction of  $\text{Li}^+$  ions with ethylene carbonate (EC): Density Functional Theory calculations. *Appl. Surf. Sci.* **2010**, 257, 1463-1468
- 25) Bhatt, M.D.; O'Dwyer, C. Density functional theory calculations for ethylene carbonate-based binary electrolyte mixtures in lithium ion batteries. *Curr. Appl. Phys.* **2014**, 14, 349-354
- 26) Martínez, L.; Andrade, R.; Birgin, E.G.; Martínez, J.M. PACKMOL: A Package for Building Initial Configurations for Molecular Dynamics Simulations. *J. Comput. Chem.* **2009**, 30, 2157-2164
- 27) Soetens, J.C.; Millot, C.; Maigret, B. Molecular Dynamics Simulation of  $\text{Li}^+\text{BF}_4^-$  in Ethylene Carbonate, Propylene Carbonate and Dimethyl Carbonate Solvents. *J. Phys. Chem. A* **1998**, 102, 1055-1061
- 28) Masia, M.; Probst, M.; Rey, R. Ethylene Carbonate- $\text{Li}^+$ : A Theoretical Study of Structural and Vibrational Properties in Gas and Liquid Phases. *J. Phys. Chem. B* **2004**, 108, 2016-2027
- 29) Katon, J.E.; Cohen, M.D. Conformational Isomerism and Oriented Polycrystal Formation of Dimethyl Carbonate. *Can. J. Chem.* **1974**, 52, 1994-1996
- 30) Katon, J.E.; Cohen, M.D. The Vibrational Spectra and Structure of Dimethyl Carbonate and its Conformational Behavior. *Can. J. Chem.* **1975**, 53, 1378-1386

- 31) Thiebaut, J.M.; Rivail, J.L.; Greffe, J.L. Dielectric Studies of non Electrolyte Solutions. *J. Chem. Soc. Faraday Trans.2* **1976**, *72*, 2024-2034
- 32) Smith, W.; Forester, T. R. Parallel macromolecular simulations and the replicated data strategy: II. The RD-SHAKE algorithm. *Comput. Phys. Commun.* **1994**, *79*, 63-77
- 33) Ryckaert, J. P.; Ciccotti, G.; Berendsen, H. J. C. Numerical integration of the Cartesian equations of motion of a system with constraints: molecular dynamics of n-alkanes. *J. Comp. Phys.* **1977**, *23*, 327-341
- 34) Allen, M. P.; Tildesley, D. J., *Computer Simulations of Liquids*, Oxford University Press, Oxford, 1987
- 35) Hoover, W. G. Canonical dynamics: Equilibrium phase-space distributions. *Phys. Rev. A* **1985**, *31*, 1695-1697
- 36) Hoover, W. G. Constant pressure equations of motion. *Phys. Rev. A* **1986**, *34*, 2499-2500
- 37) Smith, W.; Forester, T. R. DL\_POLY\_2.0: A general-purpose parallel molecular dynamics simulation package. *J. Mol. Graphics* **1996**, *14*, 136-141
- 38) Borodin, O.; Smith, G.D. Quantum Chemistry and Molecular Dynamics Simulation Study of Dimethyl Carbonate: Ethylene Carbonate Electrolytes Doped with LiPF<sub>6</sub>. *J. Phys. Chem. B* **2009**, *113*, 1763-1776
- 39) Takeuchi, M.; Kameda, Y.; Umebayashi, Y.; Ogawa, S.; Sonoda, T.; Ishiguro, S.; Fujita, M.; Sano, M. Ion-ion interactions of LiPF<sub>6</sub> and LiBF<sub>4</sub> in propylene carbonate solutions. *J. Mol. Liq.* **2009**, *148*, 99-108
- 40) Takeuchi, M.; Matubayashi, N.; Kameda, Y.; Minofar, B.; Ishiguro, S.; Umebayashi, Y. Free-Energy and Structural Analysis of Ion Solvation and Contact Ion-Pair Formation of Li<sup>+</sup> with BF<sub>4</sub><sup>-</sup> and PF<sub>6</sub><sup>-</sup> in Water and Carbonate Solvents. *J. Phys. Chem. B* **2012**, *116*, 6476-6487
- 41) Postupna, O.O.; Kolesnik, Y.V.; Kalugin, O.N.; Prezhdo, O.V. Microscopic Structure and Dynamics of LiBF<sub>4</sub> Solutions in Cyclic and Linear Carbonates. *J. Phys. Chem. B* **2011**, *115*, 14563-14571

- 42) Bhatt, M.D.; Cho, M.; Cho, K. Density Functional theory calculations and ab initio molecular dynamics simulations for diffusion of  $\text{Li}^+$  within liquid ethylene carbonate. *Modelling Simul. Mater. Sci. Eng.* **2012**, *20*, 065004
- 43) Tenney, C.M.; Cygan, R.T. Analysis of Molecular Clusters in Simulations of Lithium-Ion battery Electrolytes. *J. Phys. Chem. C* **2013**, *117*, 24673-24684
- 44) Jorn, R.; Kumar, R.; Abraham, D.P.; Voth, G.A. Atomistic Modeling of the Electrode-Electrolyte Interface in Li-Ion Energy Storage Systems: Electrolyte Structuring. *J. Phys. Chem. C* **2013**, *117*, 3747-3761
- 45) Ganesh, P.; Jiang, D.; Kent, P.R.C. Accurate Static and Dynamic Properties of Liquid Electrolytes for Li-Ion Batteries from ab initio Molecular Dynamics. *J. Phys. Chem. B* **2011**, *115*, 3085-3090
- 46) Li, T.; Balbuena, P. Theoretical Studies of Lithium Perchlorate in Ethylene Carbonate, Propylene Carbonate, and Their Mixtures. *J. Electrochem. Soc.* **1999**, *146*, 3613-3622
- 47) Skarmoutsos, I.; Dellis, D.; Samios, J. Investigation of the local composition enhancement and related dynamics in supercritical  $\text{CO}_2$ -cosolvent mixtures: The case of ethanol in  $\text{CO}_2$ . *J. Chem. Phys.* **2007**, *126*, 224503
- 48) Errington, J. R.; Debenedetti, P. G. Relationship between structural order and the anomalies of liquid water. *Nature* **2001**, *409*, 318.
- 49) Kumar, P.; Buldyrev, S. V.; Stanley, H. E. A tetrahedral entropy for water. *Proc. Natl. Acad. Sci. USA* **2009**, *106*, 22130-22134.
- 50) Guardia, E.; Skarmoutsos, I.; Masia, M. Hydrogen Bonding and Related Properties in Liquid Water: A Car-Parrinello Molecular Dynamics Simulation Study. *J. Phys. Chem. B* **2014**, DOI: 10.1021/jp507196q
- 51) von Wald Cresce, A.; Xu, K. Preferential Solvation of  $\text{Li}^+$  Directs Formation of Interphase on Graphitic Anode. *Electrochem. And Solid-State Lett.* **2011**, *14*, A154-A156.

- 52) Borodin, O. Molecular Modeling of Electrolytes. In *Electrolytes for Lithium and Lithium-Ion Batteries*; Jow, T.R.; Xu, K.; Borodin, O.; Ue, M., Eds.; Modern Aspects of Electrochemistry 58; Springer: New York, 2014, pp. 371-395.
- 53) White, A.D.; Voth, G.A. Efficient and Minimal Method to Bias Molecular Simulations with Experimental Data. *J. Chem. Theory Comput.* **2014**, *10*, 3023-3030.
- 54) Soper, A.K. Computer simulation as a tool for the interpretation of total scattering data from glasses and liquids. *Molec. Simul.* **2012**, *38*, 1171-1185.



## Tables

**Table 1:** Thermodynamical parameters and Binding energies of Li<sup>+</sup> - Solvents clusters (H and BE are in kcal/mol and S in cal mol<sup>-1</sup> K<sup>-1</sup>)

Clusters	H	BE	S
EC	-1369.29		72.80
Li <sup>+</sup> (EC)	-1293.61	-47.64	83.158
Li <sup>+</sup> (EC) <sub>2</sub>	-2698.91	-83.13	116.93
Li <sup>+</sup> (EC) <sub>3</sub>	-4090.42	-104.58	142.22
Li <sup>+</sup> (EC) <sub>4</sub>	-5473.36	-118.24	174.01
Li <sup>+</sup> (EC) <sub>5</sub>	-6849.94	-126.89	214.59
DMC	-1530.16		82.45
Li <sup>+</sup> (DMC)	-1449.02	-42.09	90.63
Li <sup>+</sup> (DMC) <sub>2</sub>	-3012.21	-73.96	124.48
Li <sup>+</sup> (DMC) <sub>3</sub>	-4562.42	-92.93	158.11
Li <sup>+</sup> (DMC) <sub>4</sub>	-6100.82	-103.18	216.80
Li <sup>+</sup> (DMC) <sub>5</sub>	-7636.69	-108.52	251.31
PC	-1736.04		79.59
Li <sup>+</sup> (PC)	-1662.22	-49.50	89.78
Li <sup>+</sup> (PC) <sub>2</sub>	-3435.12	-85.30	123.69
Li <sup>+</sup> (PC) <sub>3</sub>	-5193.16	-106.50	154.50
Li <sup>+</sup> (PC) <sub>4</sub>	-6944.97	-121.26	180.30
Li <sup>+</sup> (PC) <sub>5</sub>	-8687.22	-128.80	231.30

H=Enthalpy, BE = Binding Energy, S = Entropy

**Table 2:** Gibbs free energy of clusters (kcal/mol)

Clusters	G		
	S=EC	S=DMC	S=PC
Li <sup>+</sup> (S) + 4S	-6882.37	-7695.00	-8728.06
Li <sup>+</sup> (S) <sub>2</sub> + 3S	-6906.74	-7713.54	-8751.31
Li <sup>+</sup> (S) <sub>3</sub> + 2S	-6914.81	-7719.03	-8758.76
Li <sup>+</sup> (S) <sub>4</sub> + S	-6916.24	-7720.19	-8758.50
Li <sup>+</sup> (S) <sub>5</sub>	-6913.92	-7711.62	-8756.18

**Table 3:** Thermodynamical parameters and Binding energies of  $\text{Li}^+(\text{EC})_n(\text{DMC})_m$  ( $n+m=4$ ) clusters (H and BE are in kcal/mol and S in  $\text{cal mol}^{-1} \text{K}^{-1}$ )

Clusters	H	BE	S
$\text{Li}^+(\text{EC})_3(\text{DMC})$	-5632.24	-116.25	182.07
$\text{Li}^+(\text{EC})_2(\text{DMC})_2$	-5790.35	-113.01	186.23
$\text{Li}^+(\text{EC})(\text{DMC})_3$	-5946.18	-109.05	204.92
H=Enthalpy, BE = Binding Energy, S = Entropy			

**Table 4:** Gibbs free energies (in kcal/mol) of clusters containing two types of solvents.

Clusters	G
$\text{Li}^+(\text{EC})_3(\text{DMC}) + \text{EC} + 3 \text{ DMC}$	-11741.73
$\text{Li}^+(\text{EC})_2(\text{DMC})_2 + 2 \text{ EC} + 2 \text{ DMC}$	-11737.33
$\text{Li}^+(\text{EC})(\text{DMC})_3 + 3 \text{ EC} + 1 \text{ EC}$	-11734.99
$\text{Li}^+(\text{EC})_4 + 4 \text{ DMC}$	-11744.20
$\text{Li}^+(\text{DMC})_4 + 4 \text{ EC}$	-11729.42

**Table 5:** Thermodynamical parameters and Binding energies of  $\text{Li}^+(\text{EC})_l(\text{DMC})_m(\text{PC})_n$  ( $l+m+n=4$ ) clusters (H and BE are in kcal/mol and S in  $\text{cal mol}^{-1} \text{K}^{-1}$ )

Fragments	H	BE	S
$\text{Li}^+(\text{EC})_3(\text{DMC})(\text{PC})$	-5999.30	-116.62	188.98
$\text{Li}^+(\text{EC})(\text{DMC})_2(\text{PC})$	-6157.02	-114.01	202.51
$\text{Li}^+(\text{EC})(\text{DMC})(\text{PC})_2$	-6367.24	-117.24	188.86
H=Enthalpy, BE = Binding Energy, S = Entropy			

**Table 6:** Gibbs free energies (in kcal/mol) of clusters containing three types of solvents.

Clusters	G
$\text{Li}^+(\text{EC})_2(\text{DMC})(\text{PC}) + 2 \text{ EC} + 3 \text{ PC} + 3 \text{ DMC}$	-18781.16
$\text{Li}^+(\text{EC})(\text{DMC})_2(\text{PC}) + 3 \text{ EC} + 3 \text{ PC} + 2 \text{ DMC}$	-18779.16
$\text{Li}^+(\text{EC})(\text{DMC})(\text{PC})_2 + 3 \text{ EC} + 2 \text{ PC} + 3 \text{ DMC}$	-18780.28
$\text{Li}^+(\text{EC})_4 + 4 \text{ DMC} + 4 \text{ PC}$	-18783.28
$\text{Li}^+(\text{DMC})_4 + 4 \text{ EC} + 4 \text{ PC}$	-18768.50
$\text{Li}^+(\text{PC})_4 + 4 \text{ EC} + 4 \text{ DMC}$	-18781.65

**Table 7:** Peak positions and amplitudes of the calculated prdfs, together with the first minimum position and the corresponding coordination numbers for the first solvation shell of  $\text{Li}^+$ .

System	EC	PC	DMC	EC:DMC (1:1)	EC:DMC:PC (1:1:3)
First Peak Position- Amplitude	1.78 Å 63.19	1.78 Å 80.20	1.78 Å 85.58	<u><math>\text{Li}^+</math>-EC:</u> 1.78 Å 46.36 <u><math>\text{Li}^+</math>-DMC:</u> 1.78 Å 103.29	<u><math>\text{Li}^+</math>-EC:</u> 1.78 Å 54.51 <u><math>\text{Li}^+</math>-DMC:</u> 1.78 Å 202.09 <u><math>\text{Li}^+</math>-PC:</u> 1.78 Å 48.03
First Minimum Position	2.58 Å	2.53 Å	2.58 Å	<u><math>\text{Li}^+</math>-EC:</u> 2.53 Å <u><math>\text{Li}^+</math>-DMC:</u> 2.58 Å	<u><math>\text{Li}^+</math>-EC:</u> 2.43 Å <u><math>\text{Li}^+</math>-DMC:</u> 2.43 Å <u><math>\text{Li}^+</math>-PC:</u> 2.43 Å
Coordination Number (First Shell)	4.13	4.12	4.00	<u><math>\text{Li}^+</math>-EC:</u> 1.41 <u><math>\text{Li}^+</math>-DMC:</u> 2.66	<u><math>\text{Li}^+</math>-EC:</u> 0.58 <u><math>\text{Li}^+</math>-DMC:</u> 1.86 <u><math>\text{Li}^+</math>-PC:</u> 1.60

**Table 8:** Average values of  $q$  and  $S_{\text{tet}} / K_B$  per lithium cation obtained by the MD simulations.

System	EC	PC	DMC	EC:DMC (1:1)	EC:DMC:PC (1:1:3)
$\langle q \rangle$	0.934	0.932	0.964	0.948	0.947
$S_{\text{tet}} / K_B$	-4.56	-4.52	-5.29	-4.87	-4.84

## FIGURES

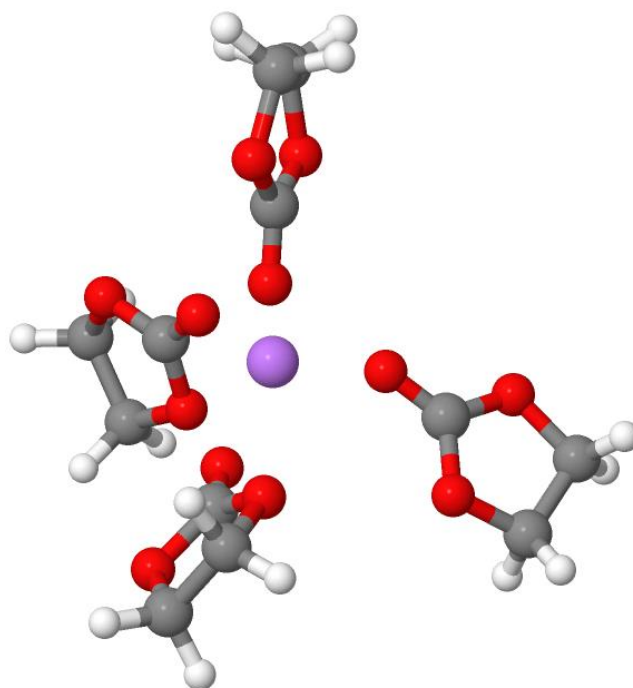


Figure 1

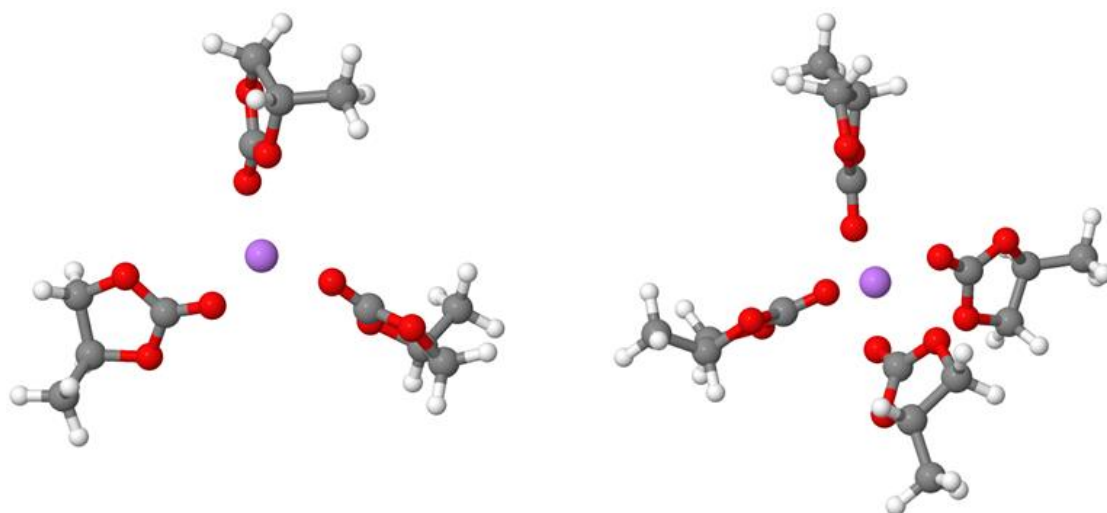
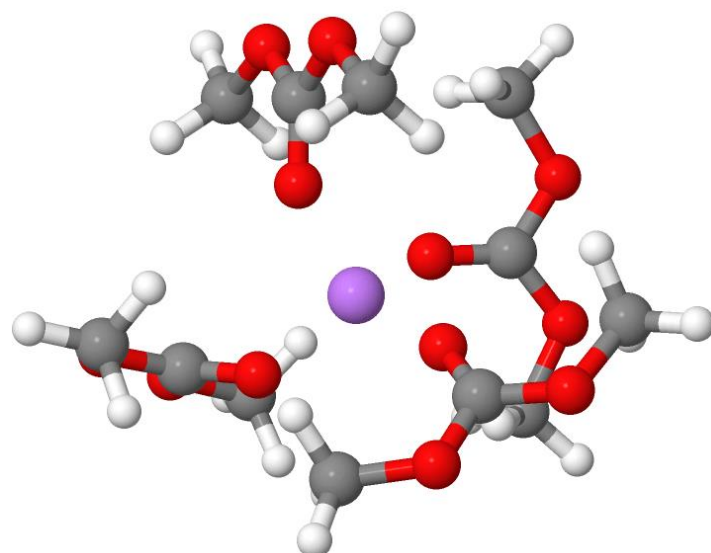
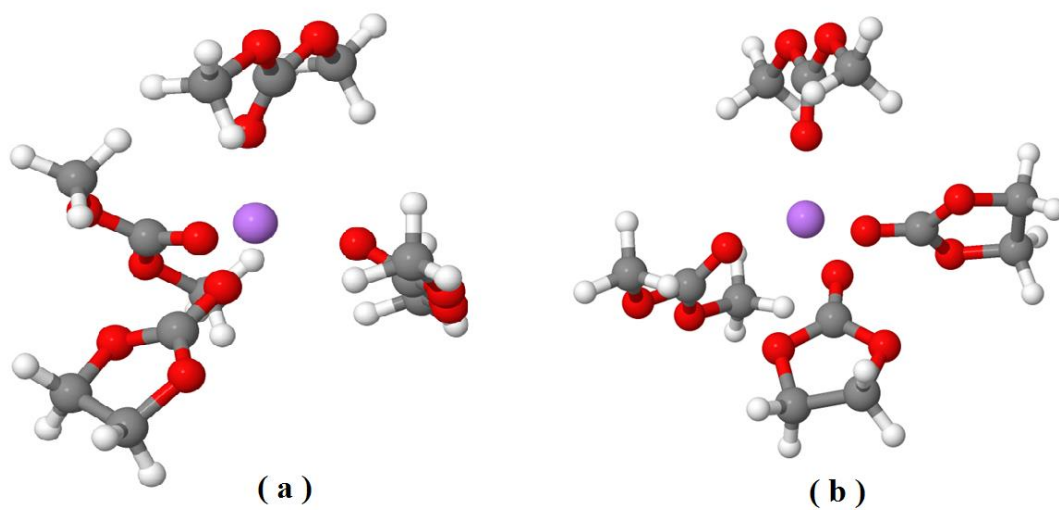


Figure 2



**Figure 3**



**Figure 4**

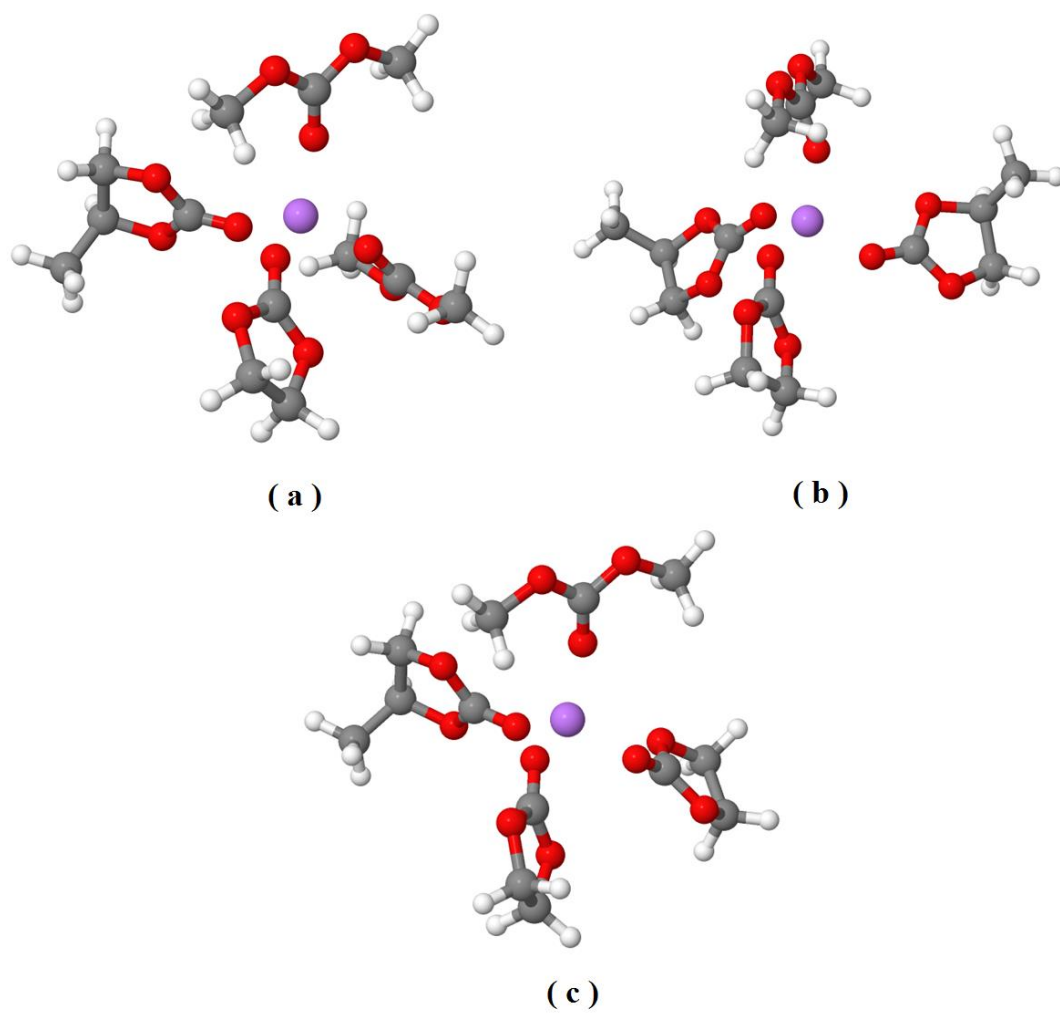


**Figure 5**

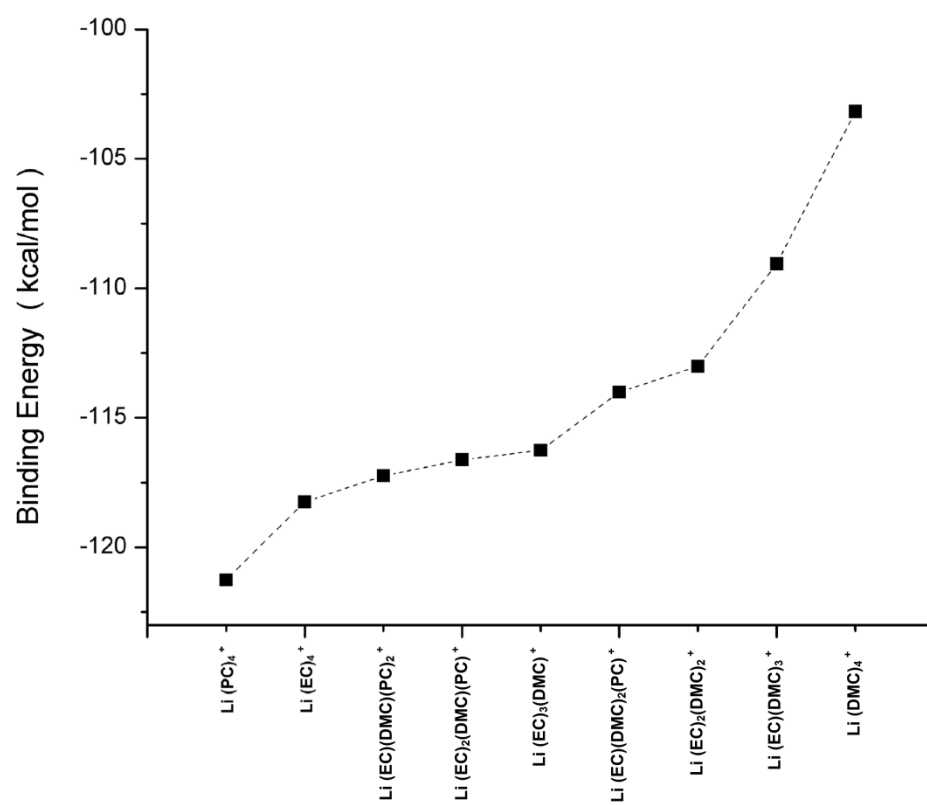
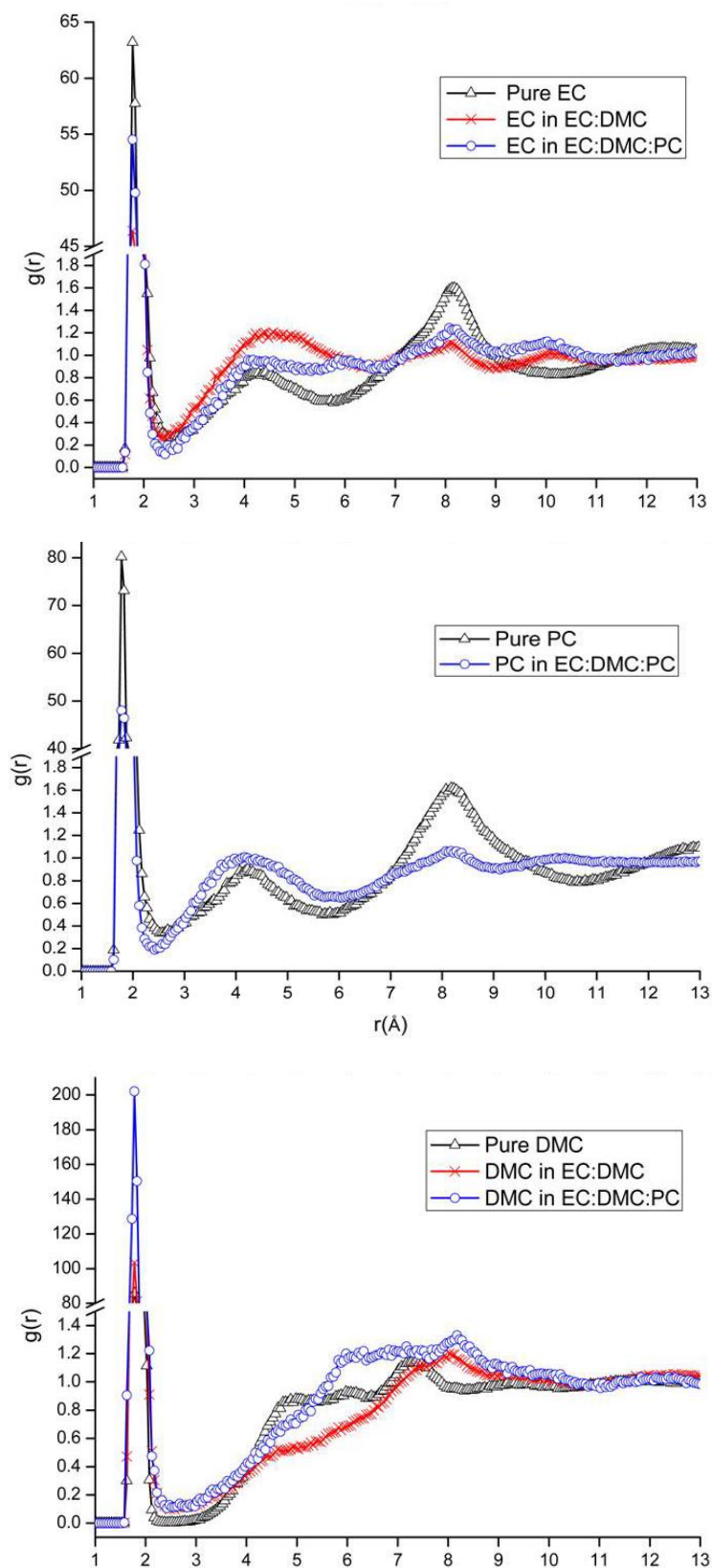
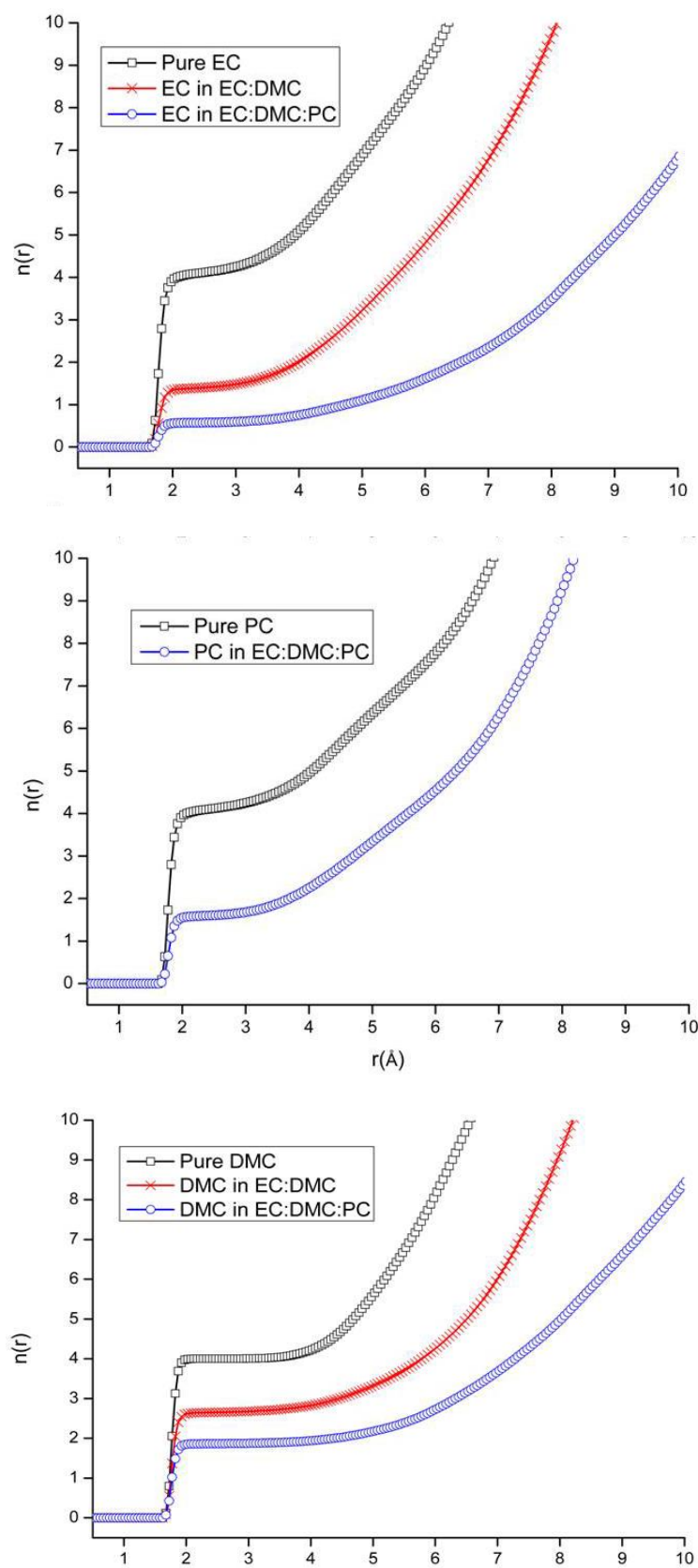


Figure 6



**Figure 7**





**Figure 8**

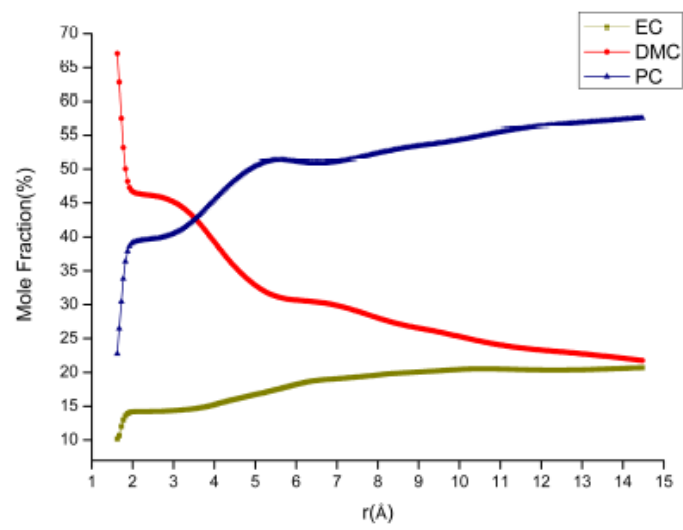
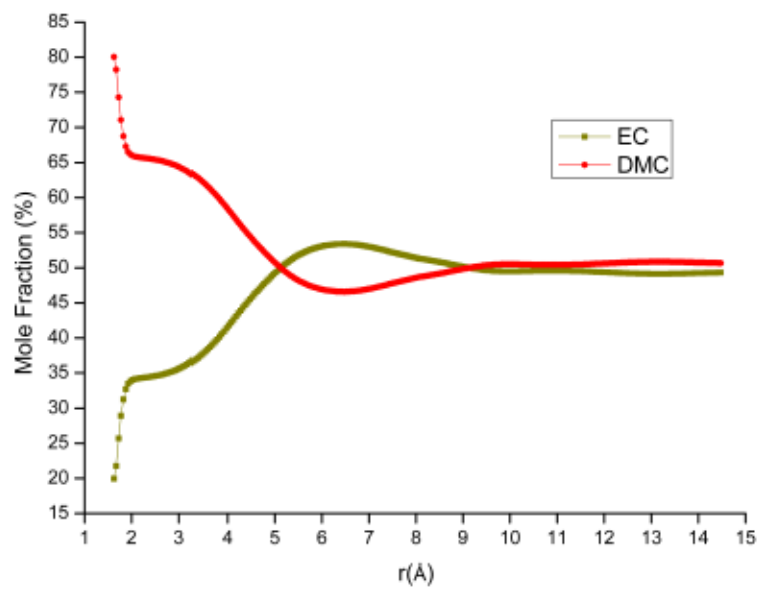


**Figure 9**

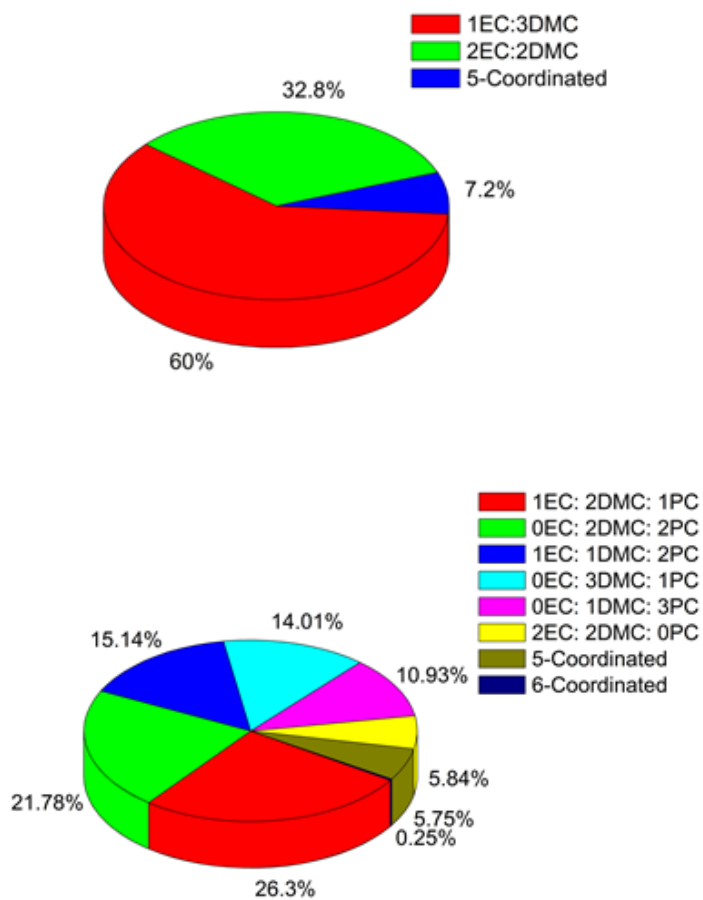


**Figure 10**

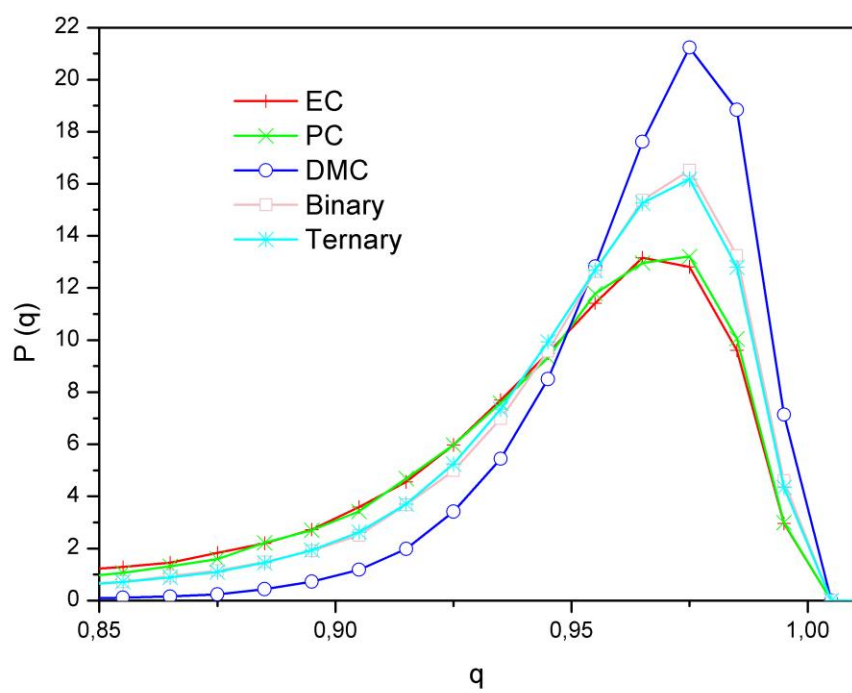


**Figure 11**

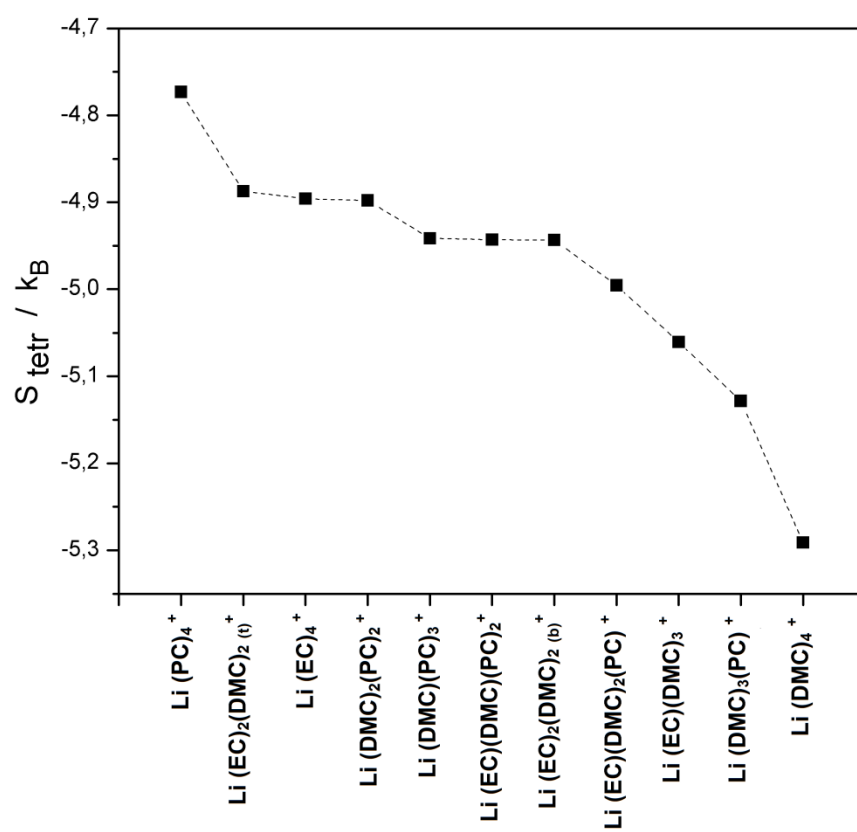
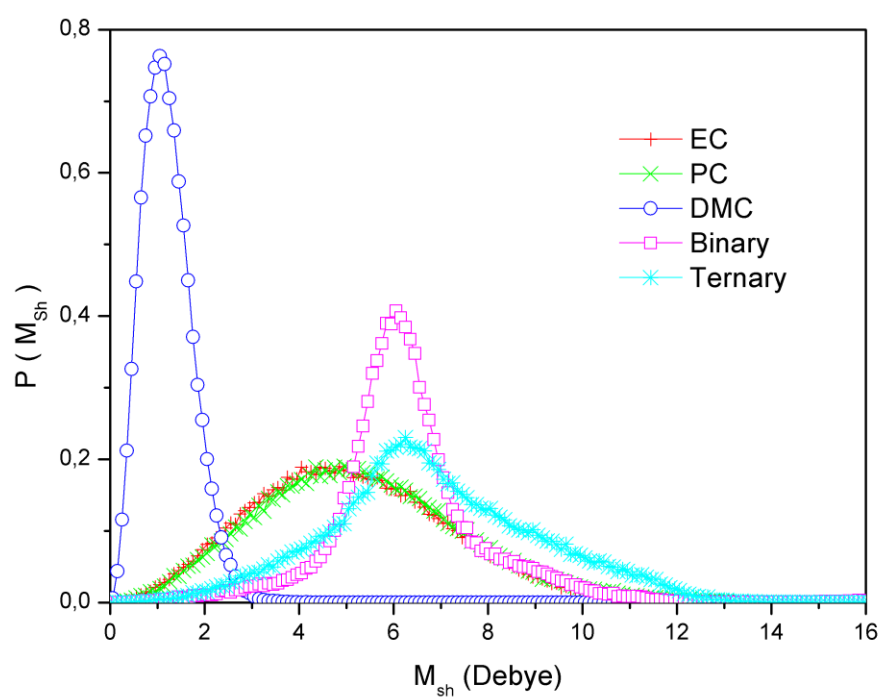


Figure 12



**Figure 13**

## Figure Captions

**Figure 1:** Structure of the optimized  $\text{Li}(\text{EC})_4^+$  cluster.

**Figure 2:** Structure of the optimized  $\text{Li}(\text{PC})_3^+$  and  $\text{Li}(\text{PC})_4^+$  clusters.

**Figure 3:** Structure of the optimized  $\text{Li}(\text{DMC})_4^+$  cluster.

**Figure 4:** Structure of the optimized: (a)  $\text{Li}(\text{EC})(\text{DMC})_3^+$  and (b)  $\text{Li}(\text{EC})_2(\text{DMC})_2^+$  clusters.

**Figure 5:** Structure of the optimized: (a)  $\text{Li}(\text{EC})(\text{PC})(\text{DMC})_2^+$ , (b)  $\text{Li}(\text{EC})(\text{PC})_2(\text{DMC})^+$  and (c)  $\text{Li}(\text{EC})_2(\text{PC})(\text{DMC})^+$  clusters.

**Figure 6:** Calculated binding energies of the optimized tetracoordinated  $\text{Li}^+$  clusters.

**Figure 7:** Calculated  $\text{Li}^+$  -  $\text{O}_c$  radial distribution functions.

**Figure 8:** Calculated  $\text{Li}^+$  -  $\text{O}_c$  local coordination numbers.

**Figure 9:** Local mole fractions (%) of EC, PC, DMC as a function of the distance from the lithium cation in the binary and ternary mixtures.

**Figure 10:** Fractions of the  $\text{Li}(\text{EC})_n(\text{DMC})_{4-n}^+$  and  $\text{Li}(\text{EC})_n(\text{PC})_m(\text{DMC})_{4-n-m}^+$  clusters in the binary and ternary mixture.

**Figure 11:** Normalized distribution of the tetrahedral order parameter around  $\text{Li}^+$  in all the investigated solvents.

**Figure 12:** The calculated values of  $S_{\text{tet}}^{nlm}$  corresponding to all the tetracoordinated  $\text{Li}^+$  clusters observed in the pure, binary and ternary solvents.

**Figure 13:** The calculated normalized probability density distributions  $P(M_{sh})$  of the magnitude of the total dipole  $M_{sh} = |\vec{M}_{sh}|$  inside the solvation shell of  $\text{Li}^+$ .

## Supporting Information

Equilibrium Geometries of EC, PC and DMC molecules used in the MD simulations.

The xyz atomic coordinates are in Å.

### EC

OC	2.059612	-0.000019	-0.000012
CC	0.862845	-0.000010	-0.000033
OR	0.075087	1.130631	-0.058017
CR	-1.318251	0.759526	0.127357
HR	-1.613656	1.016730	1.146354
HR	-1.921761	1.320441	-0.583430
CR	-1.318270	-0.759501	-0.127320
HR	-1.613707	-1.016703	-1.146308
HR	-1.921771	-1.320402	0.583486
OR	0.075066	-1.130632	0.058017

### PC

OCp	-2.323271	-0.679516	-0.136873
CCp	-1.222514	-0.222452	-0.020648
OR1	-0.926767	1.124962	-0.041106
CR1	0.515775	1.297717	-0.041828
HRp	0.836807	1.545117	-1.056849
HRp	0.765251	2.115577	0.631780
OR2	-0.075107	-0.962036	0.151878
CR2	1.055380	-0.069314	0.427027
HRp	1.202438	-0.074795	1.510600
CM	2.305958	-0.569061	-0.282629
HRp	3.144484	0.100125	-0.074580
HRp	2.573416	-1.565857	0.068179
HRp	2.151166	-0.608788	-1.361852

### DMC

CRd	-2.369295	-0.019716	0.000026
HRd	-2.464691	0.601686	0.889777
HRd	-2.464262	0.602472	-0.889241
HRd	-3.118750	-0.806456	-0.000568
ORd	-1.091531	-0.718884	-0.000136
CCd	0.000000	0.087518	0.000067
OCd	-0.000001	1.302278	0.000014
ORd	1.091532	-0.718884	0.000211
CRd	2.369296	-0.019715	-0.000092
HRd	2.464697	0.602252	0.889263
HRd	3.118751	-0.806456	-0.000192
HRd	2.464257	0.601907	-0.889756



```

EC_PC_DMC_Li  DL_POLY FIELD FILE
units kcal
molecules 4
LIT
nummols 1
atoms 1
Li          7.0000  1.0000  1
finish
EC
nummols 43
atoms 10
OC          16.0000 -0.6452  1
CC          12.0000  1.0996  1
OR          16.0000 -0.4684  1
CR          12.0000  0.0330  1
HR          1.0000  0.1041  1
HR          1.0000  0.1041  1
CR          12.0000  0.0330  1
HR          1.0000  0.1041  1
HR          1.0000  0.1041  1
OR          16.0000 -0.4684  1
rigid 1
10 1 2 3 4 5 6 7 8 9 10
finish
PC
nummols 129
atoms 13
OCp          16.0000 -0.6378  1
CCp          12.0000  1.0489  1
OR1          16.0000 -0.4509  1
CR1          12.0000 -0.0040  1
HRp          1.0000  0.1165  1
HRp          1.0000  0.1165  1
OR2          16.0000 -0.4120  1
CR2          12.0000  0.0832  1
HRp          1.0000  0.1165  1
CM          12.0000 -0.3264  1
HRp          1.0000  0.1165  1
HRp          1.0000  0.1165  1
HRp          1.0000  0.1165  1
rigid 1
13 1 2 3 4 5 6 7 8 9 10 11 12 13
finish
DMC
nummols 43
atoms 12
CRd          12.00000 -0.156100  1
HRd          1.00000  0.133100  1
HRd          1.00000  0.133100  1
HRd          1.00000  0.133100  1
ORd          16.00000 -0.447800  1
CCd          12.00000  1.086600  1
OCd          16.00000 -0.677400  1
ORd          16.00000 -0.447800  1
CRd          12.00000 -0.156100  1
HRd          1.00000  0.133100  1
HRd          1.00000  0.133100  1
HRd          1.00000  0.133100  1

```

```

constrains 11
  1    2    1.090
  1    3    1.090
  1    4    1.090
  1    5    1.457
  5    6    1.357
  6    7    1.215
  6    8    1.357
  8    9    1.457
  9   10    1.090
  9   11    1.090
  9   12    1.090

```

```

angles 17
harm  2    1    3    66.0100    107.8000
harm  2    1    4    66.0100    107.8000
harm  3    1    4    66.0100    107.8000
harm 10    9   11    66.0100    107.8000
harm 10    9   12    66.0100    107.8000
harm 11    9   12    66.0100    107.8000
harm  5    1    2    50.8000    108.6000
harm  5    1    3    50.8000    108.6000
harm  5    1    4    50.8000    108.6000
harm 10    9    8    50.8000    108.6000
harm 11    9    8    50.8000    108.6000
harm 12    9    8    50.8000    108.6000
harm  1    5    6    62.0000    108.1400
harm  9    8    6    62.0000    108.1400
harm  5    6    7    75.4000    124.9700
harm  7    6    8    75.4000    124.9700
harm  5    6    8    72.4000    110.2000

```

```

dihedrals 12
cos3   2    1    5    6    0.000000    0.000000    0.760000    0.500000    0.500000
cos3   3    1    5    6    0.000000    0.000000    0.760000    0.500000    0.500000
cos3   4    1    5    6    0.000000    0.000000    0.760000    0.500000    0.500000
cos3  10    9    8    6    0.000000    0.000000    0.760000    0.500000    0.500000
cos3  11    9    8    6    0.000000    0.000000    0.760000    0.500000    0.500000
cos3  12    9    8    6    0.000000    0.000000    0.760000    0.500000    0.500000
cos    1    5    6    7    1.400000    180.000000    1          0.500000    0.500000
cos    1    5    6    7    3.200000    180.000000    2          0.000000    0.000000
cos    9    8    6    7    1.400000    180.000000    1          0.500000    0.500000
cos    9    8    6    7    3.200000    180.000000    2          0.000000    0.000000
cos    1    5    6    8    2.700000    180.000000    2          0.500000    0.500000
cos    9    8    6    5    2.700000    180.000000    2          0.500000    0.500000

```

```

finish

```

```

vdW 190
HR     HR     lj    0.0300000    2.500
HR     CC     lj    0.0561249    3.062
HR     OR     lj    0.0714143    2.739
HR     CR     lj    0.0444972    2.958
HR     OC     lj    0.0793725    2.720
HR     Li     lj    0.0756968    1.911
CC     CC     lj    0.1050000    3.750
CC     OR     lj    0.1336039    3.354
CC     CR     lj    0.0832466    3.628
CC     OC     lj    0.1484924    3.332
CC     Li     lj    0.1416157    2.340

```

OR	OR	lj	0.1700000	3.000
OR	CR	lj	0.1059245	3.240
OR	OC	lj	0.1889444	2.980
OR	Li	lj	0.1801943	2.093
CR	CR	lj	0.0660000	3.500
CR	OC	lj	0.1177285	3.219
CR	Li	lj	0.1122765	2.261
OC	OC	lj	0.2100000	2.960
OC	Li	lj	0.2002748	2.079
Li	Li	lj	0.1910000	1.460
HRd	HRd	lj	0.0300000	2.500
HRd	CCd	lj	0.0561249	3.062
HRd	ORd	lj	0.0714143	2.739
HRd	CRd	lj	0.0444972	2.958
HRd	OCd	lj	0.0793725	2.720
HRd	Li	lj	0.0756968	1.911
CCd	CCd	lj	0.1050000	3.750
CCd	ORd	lj	0.1336039	3.354
CCd	CRd	lj	0.0832466	3.623
CCd	OCd	lj	0.1484924	3.332
CCd	Li	lj	0.1416157	2.340
ORd	ORd	lj	0.1700000	3.000
ORd	CRd	lj	0.1059245	3.240
ORd	OCd	lj	0.1889444	2.980
ORd	Li	lj	0.1801943	2.093
CRd	CRd	lj	0.0660000	3.500
CRd	OCd	lj	0.1177285	3.219
CRd	Li	lj	0.1122765	2.261
OCd	OCd	lj	0.2100000	2.960
OCd	Li	lj	0.2002748	2.079
HR	HRd	lj	0.0300000	2.500
HR	CCd	lj	0.0561249	3.062
HRd	CC	lj	0.0561249	3.062
HR	ORd	lj	0.0714143	2.739
HRd	OR	lj	0.0714143	2.739
HR	CRd	lj	0.0444972	2.958
HRd	CR	lj	0.0444972	2.958
HR	OCd	lj	0.0793725	2.720
HRd	OC	lj	0.0793725	2.720
CC	CCd	lj	0.1050000	3.750
CC	ORd	lj	0.1336039	3.354
CCd	OR	lj	0.1336039	3.354
CC	CRd	lj	0.0832466	3.623
CCd	CR	lj	0.0832466	3.623
CC	OCd	lj	0.1484924	3.332
CCd	OC	lj	0.1484924	3.332
OR	ORd	lj	0.1700000	3.000
OR	CRd	lj	0.1059245	3.240
ORd	CR	lj	0.1059245	3.240
OR	OCd	lj	0.1889444	2.980
ORd	OC	lj	0.1889444	2.980
CR	CRd	lj	0.0660000	3.500
CR	OCd	lj	0.1177285	3.219
CRd	OC	lj	0.1177285	3.219
OC	OCd	lj	0.2100000	2.960
HRp	HRp	lj	0.0300000	2.500
HRp	OCp	lj	0.0793725	2.720
HRp	CCp	lj	0.0561249	3.062

HRp	OR1	lj	0.0714143	2.739
HRp	OR2	lj	0.0714143	2.739
HRp	CR1	lj	0.0444972	2.958
HRp	CR2	lj	0.0444972	2.958
HRp	CM	lj	0.0444972	2.958
HRp	Li	lj	0.0756968	1.910
CCp	CCp	lj	0.1050000	3.750
CCp	OCp	lj	0.1484924	3.332
CCp	OR1	lj	0.1336039	3.354
CCp	OR2	lj	0.1336039	3.354
CCp	CR1	lj	0.0832466	3.623
CCp	CR2	lj	0.0832466	3.623
CCp	CM	lj	0.0832466	3.623
CCp	Li	lj	0.1416157	2.340
OR1	OR1	lj	0.1700000	3.000
OR1	OR2	lj	0.1700000	3.000
OR1	OCp	lj	0.1889444	2.980
OR1	CR1	lj	0.1059245	3.240
OR1	CR2	lj	0.1059245	3.240
OR1	CM	lj	0.1059245	3.240
OR1	Li	lj	0.1801943	2.093
OR2	OR2	lj	0.1700000	3.000
OR2	OCp	lj	0.1889444	2.980
OR2	CR1	lj	0.1059245	3.240
OR2	CR2	lj	0.1059245	3.240
OR2	CM	lj	0.1059245	3.240
OR2	Li	lj	0.1801943	2.093
CR1	CR1	lj	0.0660000	3.500
CR1	OCp	lj	0.1177285	3.219
CR1	CR2	lj	0.0660000	3.500
CR1	CM	lj	0.0660000	3.500
CR1	Li	lj	0.1122764	2.261
CR2	CR2	lj	0.0660000	3.500
CR2	OCp	lj	0.1177285	3.219
CR2	CM	lj	0.0660000	3.500
CR2	Li	lj	0.1122764	2.261
OCp	OCp	lj	0.2100000	2.960
OCp	CM	lj	0.1177285	3.219
OCp	Li	lj	0.2002748	2.079
CM	CM	lj	0.0660000	3.500
CM	Li	lj	0.1122764	2.261
HRp	HR	lj	0.0300000	2.500
HRp	OC	lj	0.0793725	2.720
HR	OCp	lj	0.0793725	2.720
HRp	CC	lj	0.0561249	3.062
HR	CCp	lj	0.0561249	3.062
HRp	OR	lj	0.0714143	2.739
HR	OR1	lj	0.0714143	2.739
HR	OR2	lj	0.0714143	2.739
HRp	CR	lj	0.0444972	2.958
HR	CR1	lj	0.0444972	2.958
HR	CR2	lj	0.0444972	2.958
HR	CM	lj	0.0444972	2.958
CCp	CC	lj	0.1050000	3.750
CCp	OC	lj	0.1484924	3.332
CC	OCp	lj	0.1484924	3.332
CCp	OR	lj	0.1336039	3.354
CC	OR1	lj	0.1336039	3.354

CC	OR2	lj	0.1336039	3.354
CCp	CR	lj	0.0832466	3.623
CC	CR1	lj	0.0832466	3.623
CC	CR2	lj	0.0832466	3.623
CC	CM	lj	0.0832466	3.623
OR	OR1	lj	0.1700000	3.000
OR	OR2	lj	0.1700000	3.000
OR1	OC	lj	0.1889444	2.980
OR2	OC	lj	0.1889444	2.980
OR	OCp	lj	0.1889444	2.980
OR	CR1	lj	0.1059245	3.240
OR1	CR	lj	0.1059245	3.240
OR2	CR	lj	0.1059245	3.240
OR	CR2	lj	0.1059245	3.240
OR	CM	lj	0.1059245	3.240
CR1	CR	lj	0.0660000	3.500
CR2	CR	lj	0.0660000	3.500
CR	OCp	lj	0.1177285	3.219
CR1	OC	lj	0.1177285	3.219
CR2	OC	lj	0.1177285	3.219
CR	CM	lj	0.0660000	3.500
OCp	OC	lj	0.2100000	2.960
OC	CM	lj	0.1177285	3.219
HRp	HRd	lj	0.0300000	2.500
HRp	OCd	lj	0.0793725	2.720
HRd	OCp	lj	0.0793725	2.720
HRp	CCd	lj	0.0561249	3.062
HRd	CCp	lj	0.0561249	3.062
HRp	ORd	lj	0.0714143	2.739
HRd	OR1	lj	0.0714143	2.739
HRd	OR2	lj	0.0714143	2.739
HRp	CRd	lj	0.0444972	2.958
HRd	CR1	lj	0.0444972	2.958
HRd	CR2	lj	0.0444972	2.958
HRd	CM	lj	0.0444972	2.958
CCp	CCd	lj	0.1050000	3.750
CCp	OCd	lj	0.1484924	3.332
CCd	OCp	lj	0.1484924	3.332
CCp	ORd	lj	0.1336039	3.354
CCd	OR1	lj	0.1336039	3.354
CCd	OR2	lj	0.1336039	3.354
CCp	CRd	lj	0.0832466	3.623
CCd	CR1	lj	0.0832466	3.623
CCd	CR2	lj	0.0832466	3.623
CCd	CM	lj	0.0832466	3.623
ORd	OR1	lj	0.1700000	3.000
ORd	OR2	lj	0.1700000	3.000
OR1	OCd	lj	0.1889444	2.980
OR2	OCd	lj	0.1889444	2.980
ORd	OCp	lj	0.1889444	2.980
ORd	CR1	lj	0.1059245	3.240
OR1	CRd	lj	0.1059245	3.240
OR2	CRd	lj	0.1059245	3.240
ORd	CR2	lj	0.1059245	3.240
ORd	CM	lj	0.1059245	3.240
CR1	CRd	lj	0.0660000	3.500
CR2	CRd	lj	0.0660000	3.500
CRd	OCp	lj	0.1177285	3.219

CR1	OCd	lj	0.1177285	3.219
CR2	OCd	lj	0.1177285	3.219
CRd	CM	lj	0.0660000	3.500
OCp	OCd	lj	0.2100000	2.960
OCd	CM	lj	0.1177285	3.219

close